IEEE Access
Multidisciplinary ⋮ Rapid Review ⋮ Open Access Journal

Received March 20, 2020, accepted April 6, 2020, date of publication April 14, 2020, date of current version April 30, 2020.

*Digital Object Identifier 10.1109/ACCESS.2020.2987849*

# Methods and Sensors for Slip Detection in Robotics: A Survey

**ROCCO A. ROMEO[1], (Member, IEEE), AND LOREDANA ZOLLO[2] (Senior Member, IEEE)**
[1]Istituto Italiano di Tecnologia, iCub Tech, 16163 Genoa, Italy
[2]Università Campus Bio-Medico di Roma, CREO Lab–Research Unit of Advanced Robotics and Human–Centred Technologies, 00128 Rome, Italy

Corresponding author: Rocco A. Romeo (rocco.romeo@iit.it)

This work was supported in part by the National Institute for Insurance against Accidents at Work (INAIL) with PPR2 Project Control of Upper-Limb Prosthesis with neural invasive interfaces under Grant CUP:E58C13000990001, and in part by the PPR AS 1/3 Project Implantable System for the Control of an Upper Limb Prosthesis with Invasive Wireless Neural Interfaces under Grant CUP:E57B16000160005.

**ABSTRACT** The perception of slip is one of the distinctive abilities of human tactile sensing. The sense of touch allows recognizing a wide set of properties of a grasped object, such as shape, weight and dimension. Based on such properties, the applied force can be accordingly regulated avoiding slip of the grasped object. Despite the great importance of tactile sensing for humans, mechatronic hands (robotic manipulators, prosthetic hands etc.) are rarely endowed with tactile feedback. The necessity to grasp objects relying on robust slip prevention algorithms is not yet corresponded in existing artificial manipulators, which are relegated to structured environments then. Numerous approaches regarding the problem of slip detection and correction have been developed especially in the last decade, resorting to a number of sensor typologies. However, no impact on the industrial market has been achieved. This paper reviews the sensors and methods so far proposed for slip prevention in artificial tactile perception, starting from more classical techniques until the latest solutions tested on robotic systems. The strengths and weaknesses of each described technique are discussed, also in relation to the sensing technologies employed. The result is a summary exploring the whole state of art and providing a perspective towards the future research directions in the sector.

**INDEX TERMS** Force, grasp, manipulation, prosthetics, robotics, sensor, slip, slippage, tactile.

## I. INTRODUCTION

The human hand emblematically represents the evolution of the human race. To have an idea of its impressing dexterity, one may think that the human hand's number of Degrees of Freedom (DoF), i.e. twenty-one, is higher than the sum of the DoFs of lower and upper limb (including wrist). No similar biological structure can be found in the *Regnum Animale* [1]. Moreover, the sense of touch is also crucial when considering the capabilities of human hand. By exploiting different kinds of sensing units, this sense allows recognizing a great quantity of properties of a touched object: roughness, shape, dimension, weight, hardness, humidity, temperature. Based on this set of properties, the human hand is able to regulate the applied force of each finger when grasping an object. This gives the hand the possibility of carrying out a fundamental action, i.e., to avoid slip when the contact condition modifies disadvantageously. A sudden movement between the finger and the object can be promptly detected by specialized receptors, which indeed transduce the mechanical information into electrical signals. Such signals are collected by peripheral nerves innervating the hand, and then transmitted to the brain very quickly. Elaboration and response, in terms of force adjustment, are quick as well, taking even less than 100 ms [2].

These skills are still difficult to reproduce into artificial systems. Industrial robotic manipulators rarely rely on tactile data [3], as artificial tactile sensors have a number of drawbacks. For instance, hysteresis and non-linearity are highly common. Although human tactile receptors embedded in human skin are hysteretic and non-linear [4], these (as well as other) drawbacks somehow complicate the use of tactile information by artificial control software. Also, high-power consumption, temperature susceptibility and difficulty in real-time elaboration of large amounts of tactile data hindered, through the past decades, the identification of one or more solutions that can have an impact on the industrial market. At the beginning of 1990s, tactile sensors were still

The associate editor coordinating the review of this manuscript and approving it for publication was Jinming Wen.

absent in the industrial domain [5], yet they were envisaged to characterize robots in a near future, allowing them to act in unstructured environments.

At the dawn of the new millennium, even though progress was reported w.r.t. the preceding decade, tactile sensing had no meaningful application in any industrial scenario [6]. Nowadays little has changed, as artificial touch remains less reliable and developed than as e.g. artificial vision [7].

As a result, although there exist commercial robots endowed with force/torque (F/T) sensors, robot manipulators are principally found in structured environments, relying on a priori knowledge rather than on active tactile sensing. In other words, robots can deal with predefined items with e.g. known mass, also measuring the contact force, but they cannot correct the grasp under unexpected circumstances. Moreover, robot sensors do not provide other tactile properties such as shape, roughness and temperature. This is in contrast with the large number of tactile sensors that can be found in literature, as witnessed by several reviews in the last years [4], [7]–[11]. Further, the combination of static and dynamic sensing is not straightforward. The detection of dynamic events like slip often requires the exploitation of a dedicated sensing unit resorting to a different transducing principle (unless using multiaxial force sensors, commonly rather bulky). A direct consequence is the difficulty to endow robotic end effectors with slip sensors, as their encumbrance can be problematic if added to the presence of e.g. a force sensor. The routing of the power and signal cables, together with the sensors embedment within the manipulator structure, represent unneglectable issues. Also, the complexity in the design of algorithms for real time functioning would rise. This applies to all domains of robotics, e.g. prosthetics.

Surprisingly, prosthetic hands are still devoid of tactile sensory systems in spite of the large prosthetic market. A recent report [12] points out the almost total lack of tactile feedback, including slip detection, in commercial prostheses. The property of detecting slip events with as fast response as to promptly react is one of the most advanced capabilities that distinguishes the human upper limb from non-human ones. Notwithstanding the considerable amount of research carried out on this topic, to provide robotic hands with reliable anti-slip perception remains unsolved. This problem gained higher attention in the latest ten years, as confirmed by the trend in the number of related scientific publications (Fig. 1). Before, academia and industry were devoting major effort towards the development of tactile sensors which were commonly unsuitable for detecting dynamic events. As a matter of fact, the first review on the topic of artificial slip sensing came out in 2013 [13]. This might be interpreted as a demoralizing statistic, given that the first attempt to mount slip sensors onto an artificial hand dates back to 1967 [14].

In light of the above considerations, the present paper intends to collect the main techniques and sensors proposed over the last decades for slip detection in robotics. The idea is to deliver a comprehensive survey of the state of the art, providing the reader with satisfactory insights about a

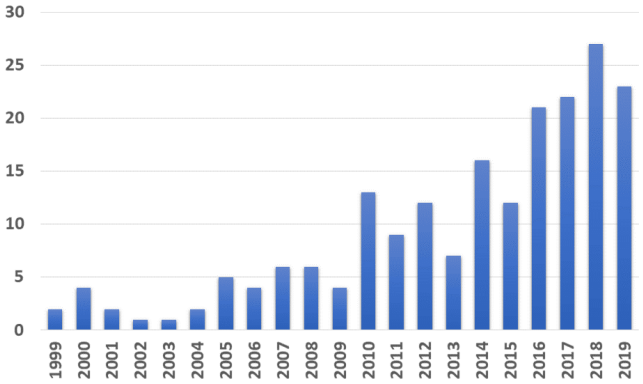


**FIGURE 1.** Number of scientific publications per year. Keywords: "Robotic slip sensor". Source: Web of Science.

field of robotics whose potential is still overly underestimated. Many of the existing reviews on tactile sensing aim at classifying tactile sensors and their potentialities; this also applies, somehow, to the reports dealing with slip detection. E.g., the aforementioned [13] focuses only on the different sensing modalities rather than on techniques and approaches. A fresher report [15] concentrates on friction estimation and on the best sensor solutions to achieve this goal.

Hence, the objective of the present paper is twofold: I) to go beyond the conventional review approach, which led to a plurality of valuable reviews focusing exclusively on sensing principles, fabrication techniques, pros and cons of the specific sensor technology and so on; II) to provide the reader with a detailed analysis of the slip detection procedures which were so far experimented in robotics, regardless of the tactile sensors involved in each work. Nevertheless, sensor technologies are cited throughout the text when explaining the various detection approaches.

We also would like to specify that all the remaining well-known problems in the state of the art of robotic grasping are not solved in the present survey. Such problems include: object drop, object damage, control algorithms for force regulation or minimization, vibration suppression, grasp stabilization, measurement of stiffness or other physical properties of the grasped object.

The article is organized in this manner: in this Section, we gave some general hints about both human and artificial tactile sensing, introducing the subproblem of slip identification, i.e. the core of the paper. The human hand constitutes a substantial inspiration for the design of robotic hands [16]: therefore, Section II briefly explains the human sense of touch, concentrating on its slip perception and correction modalities. Section III presents the methods based on the friction coefficient and on multi-axial forces, whereas Section IV deals with vibrations-based approaches. After these two Sections, which contain the majority of works, Section V offers an overview on methods resorting to other physical quantities. Section VI terminates the methods categorization by illustrating alternative approaches, including e.g. neural networks whose applications lately extended to

**TABLE 1. Basic properties of human mechanoreceptors.**

| Name | Receptor type | Field size ($mm^2$) | Encoded quantity |
|---|---|---|---|
| Meissner Corpuscles | I (fast) | 12.6 | High frequency vibrations (<50Hz) and acceleration |
| Pacinian Corpuscles | II (fast) | 101 | High frequency vibrations (>50 Hz) |
| Merkel Disks | I (slow) | 11 | Static load, skin indentation |
| Ruffini Endings | II (slow) | 59 | Skin stretch, stretch direction |

slip identification. A profound discussion of all the methods is available in Section VII; finally, Section VIII

concludes the paper and refers the authors' point of view about the future directions in this research area.

## II. HUMAN SENSE OF SLIP: PHYSIOLOGY

The human sense of touch is composed of a wide range of sensations. The human skin is commonly solicited by diverse kinds of stimuli, which might be mechanical, thermal or even electrical (e.g. electrostatic discharge, ESD). According to the nature of the stimulus, as it is delivered to the skin, one or more typologies of receptors activate. These are responsible for transducing the stimuli into electrical signals, i.e. sequences of spike potentials; such potentials are then collected by the afferent nerves, which relay them to the brain. Interestingly, the most rapid fibers (i.e. myelinated) are the ones conveying the mechanical stimuli from the related receptors, i.e. *mechanoreceptors*. These are known for their high sensitivity, thanks to which even very weak mechanical perturbations (e.g. light touch) may elicit their response. For this reason, mechanoreceptors are also called *low-threshold* receptors [17].

Table 1 summarizes the main features (retrieved from [18], [19]) of the four types of mechanoreceptors that are embedded in the human skin. It is worth mentioning that Fast Adapting (FA) units, both I and II (according to the size of the receptive field), respond only to dynamic stimulation. In particular, FA II units exhibit high sensitivity to acceleration and quick transients [20]. A similar property makes them the most adequate receptors to sense the relative movement between the hand and the grasped object. This is also due to their sensitivity to higher frequency vibrations, from 50 to 500 Hz [19] with a significant peak between 200 Hz and 300 Hz [18], [21]). When the stimulus frequency overcomes 100 Hz, displacements as little as 1 $\mu$m can lead to activation of FA II units [20]. FA I units instead produce strong firing especially for skin vibrations at frequency lower than 40 Hz and higher than 5 Hz. They are excited particularly by the skin indentation. However, it has been suggested that FA I are involved in grip adjustment when a stable grasp is disturbed with sudden loads [21], [22]. Moreover, FA I units play a role in determining the direction of the slip [13]. This information is also provided by the Slow Adapting (SA) receptors, which continue firing during static pressure but have also dynamic sensitivity. There is evidence that SA II units respond to skin stretch and have a clear directional sensitivity, as the discharge rate tended to increase/decrease when applying stretches in a direction or in the opposite one [23]. Such a property of SA II was found in animal models too [24]. Thus, SA II can be viewed as actual physiological stretch sensors. Consequently, their function can intervene in the adjustment of applied forces during tasks in which shear stresses are subject to frequent variation (e.g. tools manipulation) [18]. In other words, it is reasonable to imagine that there might be a contribution of SA II receptors in slip avoidance processes, despite their reduced sensitivity to high frequency vibrations.

The sensations related to fine touch and slip notoriously ascend to the Primary Sensory Cortex (S1) via the Dorsal Column-Median Lemniscal (DCML) pathway of the spinal cord. Before being relayed to the Central Nervous System (CNS), tactile signals need to be transduced at the skin by means of the mechanoreceptors and then sent through the peripheral nerves (e.g. forearm nerves). Once the signals are received by S1, they are elaborated and then a reaction can take place at the involved body area. Such a reaction may be faster than 100 ms, as observed in pioneering studies in the 1980s [2], [25]. Specifically, when a grasped object tends to slip, a time interval extending up to 90 ms can elapse before the first grip correction is applied. The same finding was later confirmed a decade later [26]. It is fundamental to highlight the automatic nature of the efferent signals activating the muscles in response to slip phenomena. Naturally induced slip may lead to delay in the force correction as low as around 70 ms. Conversely, voluntary reaction to externally induced stimulation of the fingers skin can produce changes in the grip forces even after 200 ms [25]. Therefore, modification in both finger position and pressure required to prevent a slip event might be regarded as spontaneous. That is, efferent signals involved in immediate reactions for slip compensation probably originate unconsciously. They are likely to be yielded by predictive strategies exploited by the CNS to perform advanced manipulation. Indeed, humans are able to store in memory information about object properties, e.g. weight, and to use such information to successfully lift the object and to eventually modify the contact conditions in order to maintain a stable grasp. However, this process resorts to visual cues as well, which are important for gaining insights about the object properties. Nonetheless, it is the tactile input that determines the entity of the error between expected sensory inputs and the real available ones. If the latter do not correspond to the former, the stored information will be updated. For more explanations about the predictive schemes underlying the skilled manipulation, see e.g. [27].

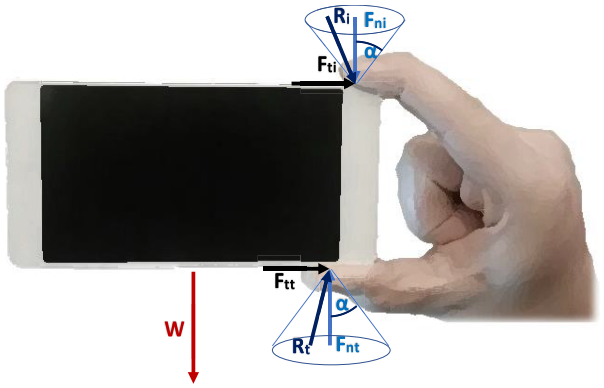


**FIGURE 2.** Forces acting on a grasped object. The two fingers apply a normal force that, in absence of any disturbance, compensates for the weight of the object. The *friction cone* must contain the resultant force vector to prevent slip. Note that the two cones have different dimensions, as the applied forces are independently applied by each finger.

## III. ROBOTICS: FRICTION COEFFICIENT AND MULTI-AXIAL FORCES

Grasp stability unavoidably depends on friction, which is a crucial element of grasp stability [15]. As a consequence, the knowledge of friction inspired multiple approaches for slip prevention. The following subsections present methods mainly based on what can be judged as a gold standard: the estimation of friction. This can be pursued e.g. by means of multi-axial force components, or else through specific sensors. Using more force sensors allows avoiding slip even without knowledge of friction.

### A. FRICTION-BASED METHODS

A fundamental parameter in the detection of slip is the static friction coefficient. The tactile receptors of human body can sense frictional variations during a grasp action, allowing the CNS to program the response in order to adjust the grasping forces. Several studies [28], [29]) have demonstrated that the applied forces are considerably conditioned by the weight of the object and the static friction coefficient $\mu_s$, which is defined as:

$$\mu_s = F_t/F_n \tag{1}$$

where $F_t$ and $F_n$ are the tangential force and normal force, respectively. If two bodies in mutual contact start moving against each other, the static friction coefficient assumes a new value $\mu_d$, which is generally lower than $\mu_s$ [30]. Equation (1) is a limit condition; to ensure stable grip of an object, the ratio $F_t/F_n$ should be lower than $\mu_s$ (Coulomb's model). Such a condition defines the *friction cone*, which must contain all the resultant forces acting on a grasped object [31]. Consider e.g. the schematization of Fig. 2. The two normal forces $F_{ni}$ and $F_{nt}$ should balance the weight $W$ of the held object in such a way that the ratio with the corresponding tangential loads $F_{ti}$ and $F_{tt}$ is littler than (1). This way, the resultant force vectors $R_i$ and $R_t$ will be located inside the cone, whose vertex semi-angle is $\alpha = tan^{-1}(\mu_s)$. If the tangential force grows until (1) holds true, the resultant force will be located on the cone surface. This would lead to *incipient* (or *initial*) slip, whereas further augmentation of tangential load would yield *global* (or *gross*) slip whenever it is not adequately compensated by increasing normal load. Referring to a practical situation in which external disturbance is missing, slip can happen if e.g. the friction coefficient (or else the object weight) is underestimated, leading to insufficient normal force. In general, given a constant $F_n$, a diminishment of the static friction coefficient is accompanied by an increment of the tangential force; these effects have to be mitigated by increasing $F_n$ to prevent object from slipping. Intuitively, the lower is the static friction coefficient, the more slippery is the corresponding surface.

Thus, the straightest methodology to prevent slip is to monitor the force ratio at the surface-object interface. This can be accomplished by measuring both the tangential and normal loads and computing their ratio. To this end, a three-axial force sensor is needed, as in [32]. This approach may be pursued through more sensing technologies, such as piezoresistive (Force Sensing Resistor, FSR, [33]) and capacitive [34]. The first technology exploits the variation of an electrical resistance produced by an exerted force, while the second is based on electrical capacitances which value depends on geometrical properties, electrical properties (such as dielectric permittivity) and to compression due to pressure. Electrical resistance variation might be exploited to sense three-axial forces with a vast quantity of fabrication processes and materials, including organic ones [35] and micro-electro mechanical systems (MEMS) [36], [37]. Capacitive sensors allow reconstructing shear forces even if the sensing unit is covered with plastic material such as silicone skin [38]. Both technologies are widely utilized in the construction of tactile sensors, though the first one is often preferred. Three-axial force sensors might be achieved by means of further transducing modalities, such as Quantum Tunnel Effect. Relevant examples can be found in [39], [40] where a Quantum Tunnel Composite (QTC) sensor capable of detecting normal and tangential forces was mounted onto an anthropomorphic mechatronic hand to provide forces information and slip correction. Notwithstanding their very high sensitivity and their high conductive behavior if pressed, QTC materials still constitute a quite uncommon solution for sensorization of artificial manipulators. Further, the detection of slip by means of three-axial force information and knowledge of the static friction coefficient was lately proposed with optical sensors [41].

The use of six-axis F/T sensors, generally relying on resistive transduction, is not rare. In [42] a six-axis sensor was mounted on the thumb of an articulated hand (i.e. Salisbury Hand) so as to measure shear and normal forces applied onto the grasped objects. In case of inconvenient variation of the friction ratio, the normal force could be augmented to prevent slip of the object. A very similar method was adopted in [30] and in [43], where the torque sensors output of a two-fingered

robot hand was used to retrieve the applied forces and to determine the friction coefficient.

The force signals provided by these sensors might also be employed in combination with other systems, e.g. cameras. This was done in [44] where a camera and a six-axis force/torque sensor were mounted on a single DOF gripper. The Hertzian model was employed; this is able to mathematically represent the contact between an elastic spherical surface and a rigid plate under the effect of a normal pressure. Such a model was extended to find out a solution for the case in which a tangential force was applied too. A slip margin $\gamma$ was defined as $\gamma = 1 - \Phi$ where $\Phi$ is equal to $F_t/\mu_s F_n$. Intuitively, when $\Phi$ is little the slip margin has a value close to one, meaning that the contact region is in a stick-state. As $\Phi$ increases, $\gamma$ becomes lower and slip is more likely to happen. The maximum value allowed for $\Phi$ is one, i.e. (1) is satisfied thus leading to object slip. The following equation was studied:

$$\delta = 3f_t\,(2-\nu)\,[1-\left(1-\Phi^{2/3}\right)]\Big/16aG\Phi, \qquad (2)$$

in which $\delta$ is the displacement of a reference point on the contact surface, $a$ is the radius of the contact area, $f_t$ is the tangential force, $\nu$ is the Poisson ratio of the elastic surface and $G$ is its shear modulus. Last two quantities are known a priori. Once $\delta$ and $a$ are estimated through the camera and $f_t$ is known thanks to the F/T sensor, two solutions $\Phi_a$ and $\Phi_b$ could be derived by solving (2) both for incipient and gross slip, respectively. Grip force can be controlled based on such solutions, thus not requiring knowledge of the static friction coefficient to prevent slip.

Additionally, torque information may be included into a stiffness control for multi-fingered manipulators, in order to maintain the grasping force within the friction cone [45]. Torques information was combined with the trend of the normal force measured by a four-axis MEMS piezoresistive sensor embedded into a soft fingertip. It was reported that normal force and moment around one of the two planar directions could provide useful insight about the onset of gross slip without the information of the static friction coefficient at the contact interface. The variation in standard deviation of torques measured by a six-axis F/T sensor integrated into the fingers of a robotic hand (Universal Robot Hand II) was utilized to predict slip in [46]. A more recent technique was proposed in [47], where a three-fingered end effector was endowed with six-axis F/T sensors to estimate the Break Away (BF) friction ratio. This was studied through the LuGre model, which considers the tiny irregularities of a surface as elastic bristles. An *applied* friction ratio depending on the disturbing force, on the normal force and object gravity was defined. The implemented controller compared the actual friction ratio $\mu_a$ with a threshold $\mu_{sl}$ obtained from normal force measurements and from the variation of the applied friction ratio. If the difference between $\mu_a$ and $\mu_{sl}$ was greater than a safety margin, the grasping force and the hand joints position were adjusted by the controller. Even though the applicability and performance of this approach were extended by the same authors [48], it suffered from certain drawbacks that will be discussed later (see Section V). Quite recent is the six-axis F/T optoelectronic sensor proposed in [49] as well, yet the slip avoidance was carried out in a classical manner, i.e. relying on (1). Two voice coil actuators, each one equipped with one sensor, were used to grasp an object, while a third actuator served to disturb it. Preliminary experiments showed the feasibility of estimating the friction coefficient and controlling grip forces through the developed optoelectronic sensors.

### B. ALTERNATIVE ESTIMATION OF FRICTION

Alternatively, it is possible to compute the friction coefficient with an ad hoc sensor, i.e. a sensor purposely conceived for this task. For instance, a clutch disk sensor was mounted on the right finger of a two-fingered robotic hand [50]. The static friction coefficient could be found as a function of the torque applied to the disk by a DC motor and of the disk radius, permitting normal force adjustment when required thanks to a force sensor based on strain gage (one sensor per finger). A singular approach was proposed in [51] with the idea of estimating the friction coefficient through an acoustic resonant tensor cell (ARTC). An ARTC sensor is composed of a cavity contained into an elastic packaging which possesses an ultrasound transmitter and a receiver. The sound propagates inside the cavity at a resonant frequency depending on the cavity shape, which in turn is influenced by the applied stresses. By knowing the vertical strain and the tangential stress of the cavity, the friction coefficient could be obtained. In this way, slip might be contrasted before it actually happened as the friction coefficient was measured without requiring any movement of the object contacting the sensor. However, to effectively use the sensor, the touched object had to be harder than the elastic sensor material and with a smaller curvature. The static friction coefficient can be inferred also by means of piezoresistive doped beams embedded in an elastomeric material [52]. The coefficient depended on the electrical resistance changes of the beams due to vertical and tangential strains met by the elastomer, whereas such stresses were proportional to the normal force.

Moreover, the ratio of normal and tangential loads exerted by a robotic finger is mathematically estimable starting from a monoaxial force information, provided that joint angles and dimensions of links are available. This was done on a fingertip mechanism constructed as in [53]. Slip was detected by observing changes in the force ratio. To compute such a ratio, more sensors are required, e.g. FSR force sensors for the monoaxial force and potentiometers for the joint angles.

### C. FRICTION-INDEPENDENT METHODS

As in some of the previously described approaches, the calculation of the static friction coefficient may be completely avoided. Structured environments, where objects properties are a priori known, do not require sophisticated algorithms for the estimation of the surface features of the manipulated objects. In this sense, the Mindlin's model offers a good

solution, allowing arithmetic prediction of the shear traction trend in the case of contact between a flexible spherical surface and a rigid flat one. The shear traction can be written as:

$$\tau(r) = 3\mu P\sqrt{(1 - r^2/a^2)}/b - 3\mu_s P_c\sqrt{(1-r^2/c^2)}/b, \quad (3)$$

where $P$ and $P_c$ are normal and critical normal load, $r$ is the radial coordinate of the contact point, $c$ is the radius of the stick area, $a$ is the radius of the whole contact area, $\mu_s$ is the static friction coefficient (known a priori) and $b = 2\pi a^2$. Even though the Mindlin's model involves $\mu_s$, we put this approach in the present Subsection as it does not require the coefficient computation. According to the model, gross slip happens when the tangential load equals the shear traction $\tau(c)$, i.e. when $r = c$ and the second part of the right term in (3) goes to zero. Pre-sliding can be detected as the tangential load reaches a critical value $\tau$' (lower than $\tau(c)$). In [54], $\tau$' was set to $0.8\tau(c)$, whereas normal and tangential forces were measured with multi-axial piezoresistive sensors inserted into some semispherical parts made of polydimethylsiloxane (PDMS). The sensors were mounted on the fingers of a robotic hand, and slip tests were performed with a ball. The model proved ability to detect both incipient and gross slip of the ball.

Further, it is possible to detect slip events analyzing the information from multiple force sensors. This is supposed to add some robustness to the sensory system but might complicate the system itself. For example, [55] performed slip detection integrating the output of a number of strain gages. A ridged structure embedding five strain gages was used as a slip sensor while additional gages positioned onto a posterior double-leaf spring structure measured normal and tangential forces, thus forming a force sensor. The increment in both the output of the slip sensor and the force ratio $F_t/F_n$ obtained through the force sensor was viewed as an indication of partial slip, i.e. the slip of only a part of the touched object (the remaining part sticks). Strain gages might also be mounted on a rubber skin to measure the strain when utilized to cover robotic fingers. If the inner side of the skin is in contact with a solid structure (*bone*) and the grasping force is insufficient, the consequent strain sensed by the gages can be addressed to the control system as a pre-slip warning. Hence, the grasping force can be increased avoiding the total slip at the external surface of the skin which holds the grasped object. Similarly, strain distribution [56] is evaluated to infer the presence of incipient slip on the surface of an elastic finger-shaped sensor. Albeit the friction coefficient is not needed, the last two approaches featured a high number of sensors (from five to fifteen gages).

Alcazar and colleagues [57] combined the signals from tactile capacitive matrices integrated in a three-fingered robotic hand (Barrett Hand). There were forty-six units on each finger and twenty-four on the palm. A convolution matrix was computed for each finger phalanx and for the palm by convoluting the current vector of raw tactile data with the previous vector (i.e. at the previous acquisition). Slip indexes were obtained based on such matrices and on the tactile units position in the array. A final slip vector was calculated by subtracting the slip indexes with the previous value, in both planar directions. Besides, the study of the gradient and rotor of such slip vectors enabled the detection of rotational slip.

In [58], the covariance matrix built on the differences $d_i$ of the recorded force at two consecutive time instants was set. A stable grasp would result in a diagonal matrix, as all covariance would be null. To do so, the infinity norm $C_\infty$ of a matrix $C$ having null diagonal and the covariances off the diagonal, was evaluated. The littler was $C_\infty$, the more stable was the grasp. A binary slip signal was generated depending on $C_\infty$. Experiments were performed on two bidigital robotic hands. The first had one FSR sensor per finger whereas the second had a $4 \times 4$ tactile array on the left finger. Grasping force could be successfully regulated, avoiding slip in the majority of the cases with both fragile and rigid objects.

## IV. VIBRATIONS

The idea to add slip measurement into artificial hands began being considered during the second half of the 1960s. Salisbury and Colman [14] integrated a piezoelectric crystal into the thumb of a mechanical hand (namely USAMBRL Hand). Baits and colleagues replicated soon after this choice on a two-dimensional gripper [59]. The purpose was, in both cases, to detect vibrations due to slip and to insert a related signal into the control loop of the manipulator. However, no experimental studies were executed to prove the capability of the so sensorized systems to detect slip. Nonetheless, vibrations generated by sliding movements between two surfaces in contact were often exploited as a slip indicator even in the successive years. The following sections describe methods that were conceived to exploit the vibration-slip relation. They were divided, in the present work, in these three main groups: piezoelectricity-based methods, frequency and time-frequency transform techniques, and filters.

### A. PIEZOELECTRICITY AND ACOUSTIC SIGNALS

Piezoelectric materials started being considered for slip detection at a very early stage in the process of robotic hands sensorization. In this context, they constitute a hugely widespread solution. The physical principle at the basis of piezoelectricity is rather intuitive. When a piezoelectric material undergoes mechanical stimulation, such as a pressure, it produces electrical charges on its opposite faces. This results in an electrical field whose voltage is associated with the exerted pressure. Such an effect is reversible, given that the application of an electrical field gives place to a deformation of the piezoelectric material.

The described physical process reminds how the human mechanoreceptors transduce mechanical stimulations into voltage signals. That is, the human skin exhibits a piezoelectric behavior [60]. This makes piezoelectric materials particularly adequate for the realization of artificial tactile sensors. Due to their large frequency response, piezoelectric tactile sensors work more easily as dynamic sensors [4].

Their sensitivity to high frequencies (even higher than 5 kHz) outperforms the one of FA II mechanoreceptors and, as a consequence, renders piezoelectricity-based tactile sensors particularly suitable for slip detection.

As already referred at the beginning of the current Section, the first attempts to endow artificial hands with piezoelectric slip sensors were done in [14], [59]. Such sensors, based on unspecified piezoelectric crystals, were expected to sense vibrations generated by the sliding of the grasped object. The signal from the sensors was fed back to the controller which could regulate the grasping forces. Mingrino *et al.* [33] employed a polyvinylidene-fluoride (PVDF, also named as PVF2) film as a dynamic sensor and mounted it on the end effector of a robotic arm (PUMA 560). Vibrations due to object motion activated the sensor, which response showed quick spikes, i.e. the slip signal. The PVDF sensor was placed above a three-axial force sensor for static force measurement (described in previous Subsection). A similar approach was followed in [61], where authors showed that the amplitude of the piezoelectric signal grew with the slip speed. Differently from [33], the PVDF transducer was collocated under a (hemispherical) three-axial force sensor. Discrimination of translational slip from rotational slip was preliminarily demonstrated, though it required the study of the curl of the tangential force measured with the force sensor.

PVDF is probably the most utilized piezoelectric polymer in the artificial slip sensing, as reported in a recent survey [62]. It was also exploited in the fabrication of synthetic ridged finger skin, of which each ridge embedded two PVDF strips [63]. Both the filtered and differentiated output of the strips were used as inputs for an artificial neural network (ANN), which decided whether the touched object was sliding or not. Designing the skin of sensorized fingertips with external nibs [64] or knobs [65] enhances the frequency response of the PVDF element.

In the new millennium, PVDF found increasing application in prosthetics. The possibility to construct flexible and low-cost sensors attracted many researchers in the last decade. Examples are illustrated in [66]–[68]. Very thin layers of PVDF ($<$100 $\mu$m) were integrated into prosthetic fingers to achieve dynamic force information. The methodology was basically common: the magnitude of the PVDF response increases when a sliding movement induces vibrations on one of its surfaces. A threshold can be applied to the voltage output of a piezoelectric sensor, as depicted in Fig. 3 [68]. Chuang and colleagues [69] proposed instead a *structural* electrode, obtained by sandwiching a PVDF layer with two flexible printed circuits (FPC). A plastic microstructure was put between the electrode surface and the polymeric encasement of the sensor to convey the applied force from the sensor surface to the PVDF element. The two microelectrodes patterned on the FPCs could detect compressive and tensile stresses when a pressure acted on the microstructure. Opposite peaks in the voltages of the two microelectrodes were judged as a slip event. The sign of the two signals provided the movement direction.

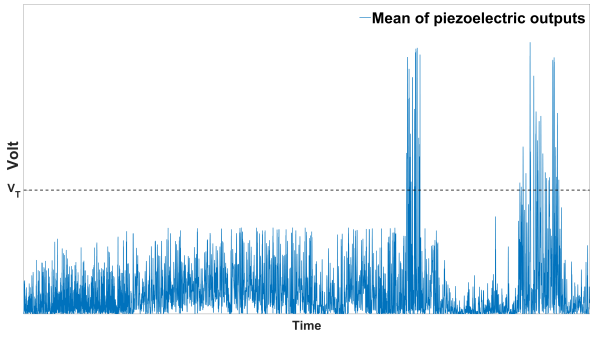


**FIGURE 3.** Signal obtained from the mean of more PVDF sensor outputs as in [68]. Peaks over threshold (dotted line) are associated with slip.

The state of the art includes some other piezoelectric materials adopted for the construction of slip sensors. The most common is the lead zirconium titanate (PZT), which belongs to the ceramic domain. This material, as the PVDF, exhibits fast voltage fluctuations when its surface moves against another one, or vice versa. Such a property was exploited in [70], where a flat bimorph PZT sensor was mounted in the distal part of a cantilever structure (acting as a fingertip) of a prosthetic hand (Southampton REMEDI Hand). Slip could be identified following the same logic as in Fig. 3. Meaningful frequency content during slip was observed in the range 200-1000 Hz. Piezoresistive (FSR) units were placed close to the PZT element in the fingertip in order to provide static force information. This approach was followed by other authors in the sensorization of myoelectrically controlled prostheses [71], [72], where slip was detected with a threshold mechanism on the rectified piezoelectric signal and contact forces were measured by FSR sensors. The sensors were not integrated in the prosthesis fingers but simply attached to them.

An older example of sensorized robotic fingertip featuring force sensors and a dynamic piezoelectric sensor is described in [73]. Here, a ceramic bimorph element was added to a piezoresistive array structure to sense microvibrations produced by slip. The piezoceramic bandwidth extended up to 500 Hz. The combination of piezoresistive (often FSR) force sensors with piezoelectric elements for dynamic events detection is frequently considered.

As an alternative, microvibrations that originate during a sliding movement might be perceived through acoustic sensors. Microphones opportunely placed below an air-filled structure are able to collect the mechanical energy released when an object slips on the structure surface. For instance, a sensor composed of a void tube and a microphone located beneath it was proposed in [74] with a myoelectric prosthesis. The so constructed sensor was mounted on the thumb of the Southampton Hand [75] and on the Oxford Intelligent Hand [76]. Vibrations at frequencies up to 1 kHz were considered significant in slip identification.

Finally, Acoustic Emission (AE) yielded by slip events may be evaluated. AE is characterized by high frequencies,

i.e. 50-1000 kHz [77], and travels within the material where it is induced in the form of elastic waves. These can be revealed by piezoelectric transducers, provided that an appropriate acoustic coupling medium is put between the transducer and the investigated material. An attempt to measure slip endowing one finger of a gripper with an AE sensor was carried out in [77]. However, acoustic and AE transducers received less attention than piezopolymers such as PVDF.

### B. TRANSFORM TECHNIQUES

Slip vibrations usually occur at high frequency. Therefore, the relating signal may be analyzed in terms of spectral features. This way, when the tactile signal shows high frequencies, an indication of incipient or gross slip can be extracted. The idea to measure slip by studying the tactile signals in the frequency domain paved the way to several works, particularly in the last decade. Although the first attempts date back to the 1990s, the availability of greater computational power in computers progressively induced researchers to privilege transformation of temporal signals into frequency signals (see Fig. 4). To this purpose, one of the most popular technique is the Fast Fourier Transform (FFT). The Cooley-Tukey algorithm [78], not covered here, is the most common FFT algorithm and allows fast computation.

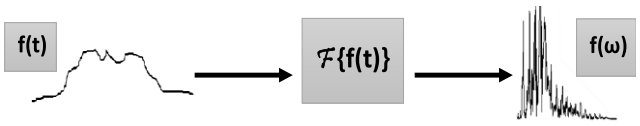


**FIGURE 4.** Basic approach for transformation of non-deterministic signals into the frequency domain. An operator, e.g. FFT, can be applied to the force signal $f(t)$ to extract its spectral content. The resulting signal $f(\omega)$ is now a function of the frequency $f$ or angular frequency $\omega = 2\pi f$.

Among the first, Holweg *et al.* [79] showed a comparison between two slip detection algorithms based on the FFT. The first one utilized the center of force distribution, calculated on the pressure outputs of a 16 × 16 piezoresistive matrix. The second performed the FFT and the Power Spectrum Density (PSD) of the normal pressure gathered from the elements of the tactile matrix. The suitability of the two algorithms was demonstrated on two different setups. In the first the tactile matrix was held still, and the object was moved between the sensor and a lever by means of a weight. In the second, a robotic gripper with sensorized fingers was horizontally translated upon a surface. Different frequency contents, achieved with and without slip, were observed. However, events quicker than 60 ms could not be detected by evaluating the changes in the center of force distribution. This was attributed to computational hardware limitation.

The FFT was reproposed several times in the following years. In [80], it was performed on the output of a tactile sensor based on strain gages. The selected time window for implementing the Cooley-Tukey algorithm was comparable with [79], i.e. 64 ms. The sensor, covered with a hemicylindrical metallic piece, allowed measuring forces along the normal and tangential directions. The tangential force appeared to be the most important in terms of high frequency fluctuations, thus the slip detection algorithm was applied onto it. Power spectrum was then computed by multiplying the FFT result by its complex conjugate and then dividing by $N$ (samples of the window).

The use of the power spectrum proved to be more reliable than the FFT when applying a threshold mechanism. The applicability of the algorithm for slip identification was demonstrated with commercial strain gages, six-axis F/T sensors of a robotic hand (Barrett Hand) and a piezoresistive tactile matrix. Another robotic hand was covered with a ridged, silicone skin embedding in the palmar area a large, flat piezoresistive FSR tactile sensor [81]. Slip was deemed to occur whenever the FSR signal peak frequency, retrieved via FFT, fell between 1 Hz and 20 Hz. The hand was controlled in such a way that the grip force was proportional to the frequency peak. Success rate in maintaining cylindrical and rectangular objects decreased with increase of sliding speed.

A technique combining statistical parameters with frequency analysis was introduced few years ago in [82]. The signals taken from two tactile arrays mounted on a robotic manipulator were used to compute the correlation coefficient. The FFT was subsequently calculated on a temporal sequence of correlation coefficients, considering slip to happen when the first frequency component was higher than an experimental threshold. In this way, slip could be inferred by observing the variation in the correlation between the two tactile sensor arrays. Statistical tools were also employed in [83], where a principal component analysis (PCA) was executed on the signals gathered from tactile piezoelectric sensors. The tactile sensors were used to sensorize the fingers of a robotic hand. The Short Time Fourier Transform (STFT) was utilized to achieve time-frequency information about the tactile signals. STFT can be regarded as a FFT shifted by a predefined window function. For each STFT obtained over eight FFTs, a feature extraction procedure was done and the features were classified with a nearest neighbor classifier. Three states could be distinguished: slip, non-slip with tactile signal and noise (no tactile signal). Very recently, the STFT was also adopted to preliminarily investigate the presence of high-frequency vibrations with FSR force sensors integrated in the thumb of a prosthetic hand [84]. Yet, the slip associated with vibrations was verified by means of the Hilbert-Huang Transform, which decomposes a given signal into a set of Intrinsic Mode Functions (IMF) thanks to an Empirical Mode Decomposition (EMD). As the first IMF overcame a pre-established threshold, a slip event was found. Furthermore, PCA was employed in [85] to select the prevailing elements of a vector composed of both frequency features, such as FFT, and temporal ones such as mean and standard deviation. All the features were computed on the three-axial force measured by a force sensor attached to the fingertips of a robotic hand.

Several works were centered on the concept of spectral power. In [86] arrays of small capacitive pressure sensors were inserted in the skin of a robotic hand. Considering the

voltage output of all the capacitive units, an estimation of the center of pressure (CoP, conceptually analogous to [79]) could be achieved. The CoP power spectrum grew as slip was automatically induced under various load and velocity conditions, on different test surfaces. Heyneman and Cutkosky outlined that signal power ratio and signal coherence are usable to distinguish between object/world slip and object/hand slip [87]. Signal power ratio was defined as the ratio between the *local power L(f,ω)* and the *ensemble power E(f, ω)*. The first was the power of the signal calculated within a given frequency band $\omega$ centered at a frequency $f$, and summed for all the sensing units in contact with an object. Conversely, the second was the sum of all the power contributions of each unit, computed in for the same frequency interval as for $L(f,\omega)$. The ratio was written as

$$\Gamma(f,\omega) = \mathrm{E}(\mathrm{f},\omega)\big/NL(f,\omega), \tag{4}$$

where $N$ is the number of units involved. The Group Square Coherence (GSC), calculated as the average of the normalized power taking into account the signal from each sensing unit, was combined with the power ratio. Results indicated good classification of object/world slip and object/hand slip in experiments on plates with various roughness and sensors (i.e. biomimetic fingertip as in [88], capacitive tactile sensors and PVDF sensors).

Another operation which lately attracted the attention of researchers is the Discrete Wavelet Transform (DWT). This transformation method decomposes the original signal into a set of subbands through a series of filters, both low-pass (LP) and high-pass (HP), yielding the so-called *approximation* coefficients and *detail* coefficients respectively. To avoid redundancy, the coefficients are subsampled by 2 at each level. This has the effect of enlarging the temporal window, thus shrinking the frequency resolution. For more extensive discussion on DWT, the reader is invited to consult [89].

The high-frequency components (details) of the DWT were exploited to detect slip events in [90] and [91]. In the first, the DWT was performed on the output of a slip sensor made of a pressure conductive rubber laying on two spiral electrodes. The sensor was mounted on a two-fingered parallel hand for experimental tests, though a supplementary force sensor (six-axis F/T) was required on one of the fingers to measure forces for grasping control. The frequency components of slip, 1 kHz or above, were identified by means of the Continuous Wavelet Transform (CWT). In the second, the DWT was instead applied on the signals of a three-axial tactile force sensors arranged into a $3 \times 3$ matrix fashion. Thus, no additional sensors for load measurement were needed. Each sensitive unit of the matrix featured a pressure conductive rubber layer, attached on an electrode substrate and covered by a PDMS dome. The thumb of a prosthetic hand was endowed with the tactile sensor to evaluate its functioning. In both works, when the high frequency signal produced by the tested sensors was greater than a threshold, slip could be revealed (even in its initial phase [90]). A slightly different approach was proposed in [92] where the DWT was computed on the output of a capacitive tactile sensor. A system comprising a dynamometer and a clamp exerted the force onto the sensor and slid several objects above the sensor surface. Rather than applying a threshold logic, the trend of the pairwise details was studied to infer the occurrence of slip. Specifically, thanks to the properties of the employed DWT (Haar Wavelet) two consecutive components of the DWT had the same absolute value but different sign. It could be distinguished the load phase from the slip phase as in the former case the sign of pairwise components switched from negative to positive, while the contrary happened in the latter case. Fig. 5 depicts the outcome of a trial.

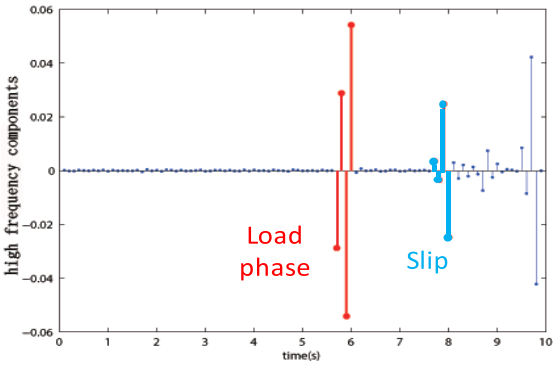


**FIGURE 5.** Pairwise high frequency components from a trial (readapted from [92]). When a load is applied onto the object, variation from negative to positive value occurs. Slip is represented by opposite variation trend.

Other publications report the use of the Haar Wavelet as a tool for slip identification in artificial hands. The DWT power can be estimated utilizing the Haar Wavelet on the same sensor as in [90], mounted on one finger of a three-finger robotic hand [93]. The adoption of a Centre of Pressure sensor avoided the necessity of using force sensors in addition to the slip one. Moreover, the wavelet coefficient energy calculated on the force signal obtained through an FSR sensor provided useful information about slip events [94]. The FSR sensor was placed on the thumb of a single DOF prosthetic hand and the wavelet signal was included into a fuzzy-logic control to manage the grasping force of the held object.

Finally, DWT is applicable on acceleration data to detect incipient slip as well as gross slip, e.g. if accelerometers are located on a prosthetic fingertip and yield high frequency outputs when relative movement with an object occurs [95]. The threshold mechanism on the DWT signal was a common element when using both DWT power and wavelet coefficient energy, as well as accelerometers.

A DWT-derived technique is the Stationary Wavelet Transform (SWT), which works similarly to the DWT except for the absence of downsampling. An up-to-date example of SWT application to slip identification is provided in [96], where a biomimetic fingertip was moved at different force and velocity levels upon naturalistic surfaces. Slip could be found with very high accuracy, regardless the experimental conditions (i.e. varying velocity and exerted force), thus

suggesting the SWT as an effective tool to solve the problem of slip detection.

Notwithstanding the DWT can be viewed as a sequence of filtering operations, it was chosen to deal with DWT-based methods in the present subsection together with the other transform operations. The next subsection will summarize approaches relying on filter functions.

### C. FILTERS

In the previous subsections, the concept of high frequency vibrations as indicator of slip emerged. During the last ten years, a further manner to extract such vibrations arose. It consists in filtering the tactile signal with purposely designed functions or circuits. Cut-off frequencies and filters order should be carefully defined to enhance the signal components within a certain band.

Being the slip frequency content much richer at high values of frequency, the most convenient way to conceive a filter is to penalize low frequencies. These usually prevail when slip does not occur; hence, HP filters do appropriately fit this task. However, band-pass (BP) filters are also suitable as they allow selecting only a particular range of frequency. Very subtle bandwidth might be chosen in order to discern meaningful frequencies from the rest of the spectrum. Probably due to this property, they were chosen more often with respect to the HP filters. In this concern, in [97] a flexible, piezoresistive tactile sensor based on conductive nanocomposite (carbon nanotubes, CNT) was developed and used for force and slip measurement. Slip events could be identified by filtering out from the sensor output all the frequencies higher than 45 Hz and lower than 40, as the most accentuated difference between signals of slip and nonslip events was observed in a very narrow band (i.e. 40-45 Hz). To this purpose, a fourth-order BP Chebyshev filter was implemented. Obviously, higher orders correspond to higher efficacy of the filter, though its complexity increases. For example, [98] illustrates a control scheme of a prosthetic hand (Motion Control Hand) based on a network composed of seven fourth-order BP filters. Each filter resonated at frequencies in the interval 20-50 Hz, with a 5 Hz pace. In this way, it was possible to isolate the slip frequencies from the tangential force signal of some strain gages located on the thumb of the prosthetic hand (covered with a cosmetic glove). A LP filter was added to the seven fourth-order functions so as to penalize frequencies above the meaningful bandwidth. This was identified through FFT of the force signals, as well as in the previously described work [97]. In both cases, the absolute value of the filtered signals was computed to obtain a monopolar signal, and then sent to the control. Force signal filtering was performed in [99] as well. Two jaw grippers (mounted on the arms of a PR2 robot), whose fingers featured a tactile matrix, were used to execute grasp experiments with a broad set of objects. To ensure slip avoidance, the force values $f_n$ from all the matrix elements (twenty-two) were HP filtered and summed, achieving the following index (readapted for sake of simplicity):

$$F_f = \sum_{n=1}^{15} H_{hp}(z) f_n, \tag{5}$$

where $H_{hp}(z)$ is the Butterworth filtering function designed to cut off frequencies below 5 Hz from the force signals. This was done for both the gripper fingers. Only the sensing elements placed in the main surface of the gripper, i.e. fifteen, were included in the calculation of $F_f$. Additionally, the force summation was filtered with a Chebyshev BP filter from 1 to 5 Hz in order to reduce the influence of too quick force variation. A slip event was detected whether $F_f$ was higher than a threshold (depending on the force summation) and, contemporarily, the BP signal was lower than an empirical threshold.

Higher frequencies were accounted for in [88], where the pressure signal from two biomimetic fingertips was filtered in the band 60-700 Hz. Subsequently, the absolute value of the filtered signal was compared with the signals of an inertial measurement unit (IMU) in terms of latency from the slip onset. The filter-based detection offered better performance than the IMU (attached to the tested objects). This was probably due to the textured skin covering the fingertips, which contained a conductive fluid. Textures with very small pace were responsible for the high frequency vibrations of the fluid; such vibrations were relayed to the pressure transducer when the touched object started slipping against the fingertips surface. Interestingly, rotational slip could be distinguished from linear slip through a neural network with 80% accuracy.

Lately, filter networks were also exploited in [100]. A robotic finger was endowed with a biomimetic fingertip featuring four MEMS tactile sensors, which in turn had four sensitive units (i.e. sixteen channels). Filtering stage included a fourth-order Butterworth BP filter, with the two cutoff frequencies at 10 Hz and 50 Hz. Two additional stopband (SB) filters were cascaded to the BP filter to attenuate all the useless frequency content, e.g. due to contact of the fingertip before the sliding movement. The filtered signal was rectified to make it unipolar; exponentiation was also performed in order to augment the difference between the portion of signal associated with slip and the peaks due to false positives (contact and release). Finally, the signal was enveloped with a 40-ms window to eliminate the quick and discontinuous spikes, achieving a smooth curve. The result of the various computational blocks is given in Fig. 6 for a test signal. All the sixteen outputs were jointly analyzed with logic operators. A final ON/OFF signal was obtained through a threshold mechanism on the enveloped signals. 100% in slip detection was achieved, whereas only around 1% of false positives in the worst case. The algorithm was formerly evaluated in a simpler configuration [101]. A single, second-order HP filter was built to cut off frequencies below 700 Hz from the normal force signal gathered by an FSR sensor, acting as a force/slip sensor. Such a sensor was placed on the index of a mechatronic hand (IH2 Hand), while two other FSR sensors

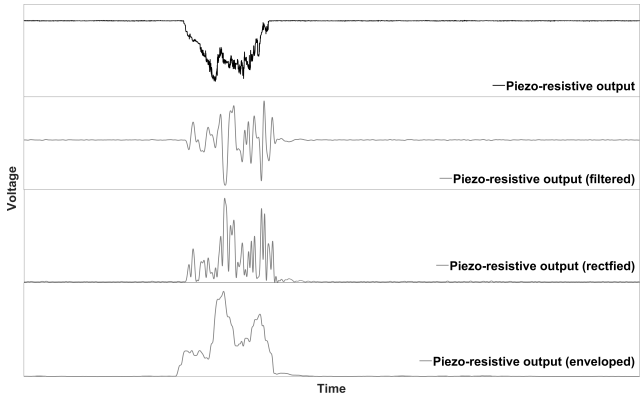


**FIGURE 6.** Signal elaboration according to [100].

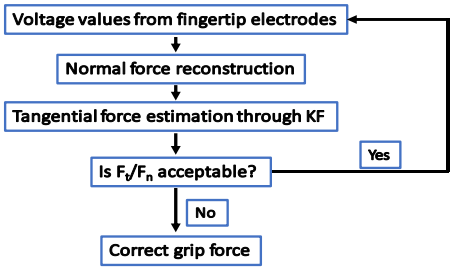


**FIGURE 7.** Flow chart of the algorithm developed in [104] (readapted). Normal force was reconstructed from the fingertip electrodes output. Tangential force was estimated on the electrodes output through the KF. Force ratio determined whether to correct the grip force or not.

were placed on the thumb and middle fingers for force measurement only. The ON/OFF signal was fed back to the hand control, which increased the grip force avoiding the grasped objects (e.g. egg and plastic cup) fall when automatically disturbed by the end effector of a robotic arm. In this work, an ad hoc hardware, i.e. a PCB, was devoted to the algorithm implementation. A further development of this method was successfully employed in an in-vivo experimentation [102].

Likewise, an ON/FF signal was generated by means of a purposely designed chip in [103]. The chip architecture was based on circuits composed of a number of silicon retinas (ST), whose transfer function was comparable with the one of a HP filter. STs are 2-D arrays of processing elements. Such elements are locally interconnected and are able to sense microvibrations and to carry out real-time processing. The chip functioning was proven on the raw force signal from a linear array of sixteen piezoresistive sensors.

A filtering tool which lately draw the attention of some researchers for the realization of slip prevention algorithm is the Kalman Filter (KF). It allows measuring unknown variables based on previous estimations which are affected by a certain amount of noise. As such, it can be regarded as a statistical tool. Remarkably, the KF works properly on dynamic systems, usually linear, and hence might be used to observe the dynamic behavior of rapidly changing quantities. Therefore, over the last years, KF filters began being considered for slip identification in the robotic field, especially in prosthetics. Wettels and colleagues utilized a KF in a classical framework, retrieving both tangential and normal forces by means of a biomimetic tactile sensor array [104]. The array was integrated into the thumb of an anthropomorphic robotic hand (Ottobock M2), forming an antecedent version of the biomimetic fingertip used in [88]. The KF took inputs from four electrodes (i.e. voltage) of the fingertip core, whereas a fifth input was given by the previous value of the tangential force. Once the tangential force was estimated through the KF, the force ratio was computed as in (1) being the normal force arithmetically reconstructed through the electrodes voltage output. Adjustments in grasping actions were carried out according to the force ratio; a Styrofoam cup was correctly handled even when rapidly filled with water. Schematization of the algorithm is drawn in Fig. 7.

Furthermore, slip identification was possible utilizing the residual of KFs applied to the tangential component of the applied force. In [105], an optoelectronic six-axis tactile sensor was employed to perform incipient slip detection. The KF residual was integrated with the Tustin's method. The static friction coefficient was also involved in the KF residual analysis, and was obtained by means of an exploring phase of the surface object. Likewise, friction coefficient estimation and KF residual were combined to infer slip occurrence in [106]. KF residual was this time LP filtered (5 Hz cut-off) to achieve a slip signal, which was compared with a threshold. The algorithm was tested on a commercial six-axis F/T sensor. Extensive dissertation about KFs is findable in [107].

## V. PHYSICAL QUANTITIES

Slip can be inferred from physical quantities relating to peculiar physical phenomena, which have to be observed with proper sensors. Piezoelectricity-based transducers were referred in the precedent Section as they represent a consolidated solution for slip detection, and strongly depend on vibrations. Here, we report works investigating the additional physical quantities that might relate to slip.

### A. OPTICS

The investigation of optical sensors as slip sensors initiated during late 80s. Hopkins and collaborators [108] suggested that macropixels, i.e. groups of single pixels captured with RAM cameras, were able to reduce computational times, storage memory required and noise (given the filtering effect of averaging many pixels). The basic idea was to compare the output of such macropixels and to recognize slip as a certain difference appeared in such an output. To do so, the camera collected the light reflected by a photoelastic element with a reflective layer, against which the object was slid. Photoelasticity was also used in [109], however the emitted light hitting the photoelastic layer was not reflected but rather caught by a receiver with a modified intensity. This descends from the fact that light is divided into some components following the directions of the so called principal stresses, originated when an external load is applied onto the photoelastic material.

The intensity of the received light is expressible as a function of the principal stresses, which in turn are function of normal and tangential loads. Hence, said intensity is modified by the object slip, as it yields variation in such stresses. Disadvantageously, if the principal stresses remain constant during the object slip, this one cannot be observed.

In [110], a hemispherical optical sensor was built featuring concentric rubber ridges, with an optical fiber positioned in each groove between two adjacent ridges. The developed sensor had sixteen fibers providing as many channels. Experiments were performed mounting the sensor on one side of a gripper interfaced with a PUMA 560 robotic arm, which lifted an object and gradually released it. Light intensity in the fibers changed as a ridge deformation, even partial, occurred during contact with the object. Slip was detected before it could totally happen in 85% of cases.

Further, optical sensors were integrated in the fingertips of a robotic hand (DLR/HIT) connected to the right arm of a mobile robotic platform (TUM-Rosie) [111]. The sensor consisted of a miniature camera and a laser emitter, and a microcontroller was dedicated to computation. The so equipped fingertip permitted recognition of slip events when the grasped object surface translated w.r.t. the sensor lens.

Other sensors comprising a camera and a light source are available: one is the GelSight. This has an elastomeric body covered with an opaque membrane which reflects the light, allowing to reconstruct the geometry of the contacted surface. In a recent version [112] tested on a gripper, the membrane was provided with randomly distributed markers which could track the deformation of the elastomer. The displacement tracked by means of the markers correlated with the shear force during grasping of items, e.g. a metallic can. Regions of pre-slip and total slip could be identified studying the entropy of the shear field magnitude. Besides, Ito *et al.* [113] showed a tactile sensor which could detect slip events by collecting images through a CCD camera. The images were obtained as the light emitted from a LED was captured by the camera after being reflected by contacted objects. A spherical, transparent body of silicone rubber acted as a contact mean; such a body was patterned with a 21 $\times$ 21 matrix of dots. Checking the brightness of each recorded pixel allowed understanding which rubber area was in contact with a certain object, and a stick ratio could be calculated. The displacement of the dots w.r.t. a reference dot was studied to localize the slip region. The stick ratio $R$ was defined as $N_s/N_c$, where $N_c$ was the number of dots enclosed by the contact region and $N_s$ was the quantity of dots for which $|d_k\text{-}d_{ref}| < \tau$. That is, if the difference between the displacement $d_{ref}$ of the reference dot and of the *k-th* dot $d_k$ was smaller than a threshold $\tau$, this dot was then aggregated to $N_s$. Additionally, tangential load, normal load and to the moment around normal axis could be retrieved from dots displacement. Very recently, a camera was used to monitor the position of some pins located hexagonally in an optical tactile sensor [114]. Such a sensor was interfaced to a robotic arm (UR5); the position of the pins was processed in real time through a support vector machine (SVM) classifier to analyze the slip presence as the sensor contacted a test object.

Another technique employing a sensor made with one photodiode (PD) and two phototransistors (PT) was presented in [115]. The infrared light emitted by the PD is reflected by an object and then gathered by the PTs. Forces were sensed with a pressure sensitive rubber, which completed the sensor structure. By computing the cross-correlation between the voltage outputs of the two transistors, slip velocity was retrieved and the applied force was corrected proportionally to such a velocity. A drawback concerning this sensor resided in that it allowed measuring movements only of polychromatic and patterned surfaces.

An optical sensor comprised of a LED and a PT was mounted on the middle finger of a prosthetic hand (i-Limb), which was in turn interfaced to a robotic arm [116]. The raw data from the sensor were first LP-filtered at a rather low frequency (i.e. 10 Hz) to reduce noise, and the difference between two consecutive filtered samples was continuously stored and summed to the previous difference value, being the initial difference set to 0. When such a sum was higher than a threshold, a spike signaling slip was generated. The threshold was dynamically adapted basing on the difference of each pair of consecutive samples. This algorithm produced good response time in slip detection when the hand was grasping a bottle gradually filled with 500 ml of water.

Finally, we report the PapillArray slip sensor [117], which consisted of a silicone pillar mimicking the papillae in the human finger pad skin. The pillar had a 15-mm diameter and a 20-mm height: it was constructed with an inner cavity hosting a diffusive reflector illuminated by two LEDs installed on the opposite side of the cavity. Between the LEDs there was a pinhole aperture, below which a quadrant PD collects the inverted image projected by the reflector. The PD signals were mapped into 3D force and displacement.

### B. VELOCITY AND ACCELERATION

Intending slip as a movement, its detection can be associated to the detection of a velocity. A Laser Doppler Velocimeter (LDV) was adopted in [118], whose principal components were a laser diode (LD), a PD and micromirrors. The LDV had very little dimensions: 7.8 mm$^2$ large and 1 mm thick. The two laser beams, emitted from the LD and reflected by the micromirrors (made of aurum), were scattered by the slipping object and then collected by the PD. By observing the resultant shifts of the peak frequency in the PD voltage, velocities from 10 $\mu$m up to 2 cm/s could be caught. The movement of plastic, metallic and cardboard objects was produced by means of a voice coil actuator. However, the tested objects were not in contact with the LDV, but simply put in front of it. This does not represent a proper slip condition.

Not only velocity but acceleration as well was exploited to get insight about slip. Howe and Cutkosky [119] probably presented the first accelerometric slip sensor for robotics in 1989, while [32], [120] showed few years later the first applications in robotic manipulation. A central foam rubber

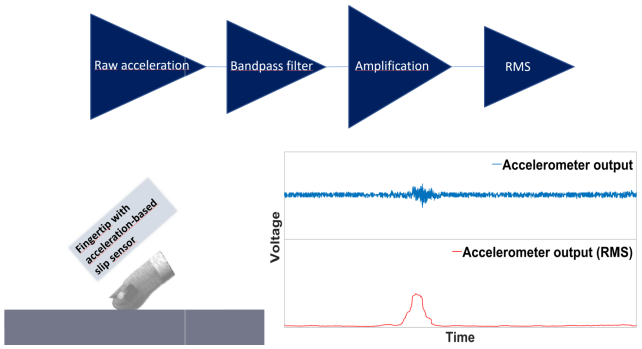


**FIGURE 8.** Elaboration of an acceleration signal from a slip sensor as in [120]. The raw output can be band-pass filtered to cut off undesired frequencies. Subsequently, amplification and calculation of RMS are reasonable steps.

was covered with a rubber skin endowed with small protuberances enhancing vibrations during slip. Such vibrations activated the accelerometer placed on the inner side of the skin, in the contact region. A slip sensor was thus obtained, and mounted on a two DOFs robotic finger. The RMS of the sensor output was used as a slip signal, obtained after filtering and amplifying the raw acceleration as depicted in Fig. 8. By gradually reducing the force exerted by the fingertip against an object (attached with a mass) until slip occurred, the sensor capabilities were tested with several materials, e.g. sandpaper, smooth paper and Teflon [120]. Wet surfaces did not worsen the sensor performance, contrarily oiled objects could not generate slip signals. Reference [32] described an improved version of the slip sensor, in which an accelerometer was added on the side of the rubber foam in the fingertip core. In this manner, noisy signals at the skin could be more easily discarded whereas vibrations due to sliding could be sensed by the side accelerometer. Similar experiments were conducted but only with a Teflon piece covered with sandpaper. Plus, a three-axial force sensor was placed behind the fingertip embedding the slip sensor, through which the friction coefficient was constantly updated for optimal grip (see Subecton III.A).

Although first demonstrations were encouraging, few other works adopted accelerometers as slip sensors in artificial manipulation. Previously mentioned articles [71], [95] made use of acceleration to detect slip events. DWT on accelerometers output positioned on a fingertip was computed in the first; the amplitude of such an output was instead checked together with the output of a PZT sensor in the second, where both the accelerometer and piezoelectric units were attached to the thumb surface. All the acceleration-based methods listed so far foresaw to implement threshold mechanisms.

Differently, in [121] the acceleration information was merely used to confirm pre-slip and gross slip sensed by an acoustic pressure transducer. The end-effector of a robotic arm, composed of two rectangular, flat fingers, was provided with both the pressure transducer and the accelerometer. Experiments regarded the grasping of a cork ball and a glass bottle. Gross slip was also perceived with an accelerometer integrated in a sensorized prosthetic finger [122].

Note that, even though some acceleration-based methods resort to vibrations, this does not apply to all of them. Therefore, we chose to place such methods in the present Section, dedicated to physical quantities in general.

### C. THERMAL, MAGNETIC AND OTHERS

In this work, quantities adopted more sporadically are treated as well, for the sake of completeness. E.g., few attempts were done with thermal sensors as well. When slip occurs between two surfaces, an amount of convective heat is released and could be marked as a slip index. This principle was adopted in [123], where a thermal probe was electrically kept at a constant temperature through a microheater. The heat $q$ generated by the probe is modellable through the Fourier equation:

$$q = \delta T/\delta t + v\nabla T - \alpha\nabla^2 T \tag{6}$$

in which $T$ is the temperature, $v$ is the slip velocity and $\alpha$ is the thermal diffusivity of the slipping body. When fast relative movements (i.e. slip) took place, heat was convectively dissipated according to the term $v\nabla T$. Heat dissipation was compensated by increasing the power supplied to the probe. A temperature threshold, above which slip was signaled, was established. Albeit it was possible to detect slip regardless the material roughness (on plastic and wood), the sensor failed to discard contact events from actual slip. A basically equivalent slip identification method and sensor, this time grounded on a flexible substrate, was illustrated in [124].

Magnetic tactile sensors were also developed to sense force and slip. A way to create a magnetic force sensor is to assembly a deformable medium together with a rigid medium [125]. The first hosted a permanent magnet at its center, while the second embedded four chip inductors. A displacement of the magnet yielded by a pressure applied on the deformable medium induced voltage in the inductors. Such a voltage depended on the variation of the magnetic flux, which in turn could be expressed as a three-dimensional space-varying function. Hence, appropriate integration of the magnetic flux allowed reconstructing three-axial force. The voltage $V_i$ in each inductor was linked to the vertical component of the magnetic flux $B_{zi}$ as follows:

$$\begin{aligned} V_i &= -M\delta B_{zi}/\delta t \\ &= -M\delta(a\sqrt{(x_i+\Delta x)^2+(y_i+\Delta y)^2}+b)/\delta t. \end{aligned} \tag{7}$$

In (7), $M = NA$ is the product of the number of coils $N$ and the coil area $A$ of the *i-th* inductor, whereas $\Delta x$ and $\Delta y$ indicate the displacement of the permanent magnet w.r.t. to the inductor position denoted by $x_i$ and $y_i$. The constants $a$ and $b$ depended on the displacement along the normal direction. Slip could be identified as a fast, prominent peak in the four induced voltages (one per inductor) during experimental tests done on a linear rail. The same sensor was modified by adding four giant magnetoresistances (GMR) in the substrate hosting the inductors [126]. GMRs voltage output served to estimate

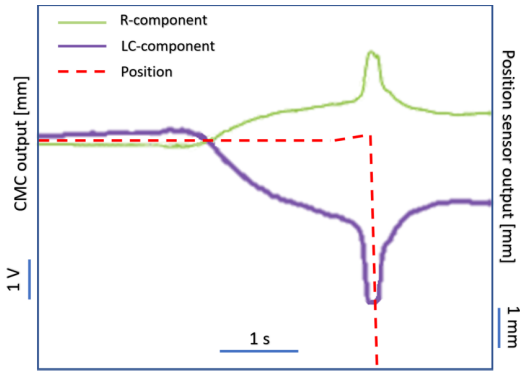


**FIGURE 9.** CMC sensor output for a typical trial. Both R-component and LC-component showed sudden variation when slip occurred. Readapted from [128].

the three-axial force while slip was detected as in the previous work. A later magnetic tactile sensor [127], recalling the one of [125] in terms of structure and functioning, was proposed for stick-slip identification as well. It confirmed the capability of the inductors voltage to exhibit significant peaks when the stick slip led to friction force variation.

A dome-shaped silicon rubber sensor, including tiny carbon coils (10 $\mu$m diameter), was used in [128]. Deformation of the so composed sensor, i.e. Carbon Micro-Coil (CMC) sensor, produced an LCR behavior, which could be quantified in terms of amplitude and phase. When the sensor was mechanically stimulated, impedance changed in both the R component and the LC component. Peaks greater than a threshold in their voltages revealed the occurrence of slip (Fig. 9).

A method based on the CoP analysis was illustrated in [129]. Unlike previously mentioned articles where the study of the CoP was conducted with spectral techniques, here the voltage output of a CoP sensor was directly observed to find correlation with slip events in the time domain. The sensor was made of two conductive sheets sandwiching a pressure sensitive layer. All materials were flexible; thus, two sensors could be wrapped around the two cylindrical fingers of a robotic gripper for experimental tests. The voltage output was inserted into the control loop of the gripper. If significant drop in such a voltage was found, the gripper increased the applied force. Slip was prevented with objects of diverse mass, though disturbance was generated manually.

Furthermore, pneumatic devices are eligible for slip detection. A pneumatic tactile sensor for sensing roughness, hardness and slip was shown in [130]. The sensor was composed of a latex tube acting as an air bladder, inside which a pressure transducer measured the pressure changes due to external forces on the tube surface. The tube was protected with a plastic parallelepiped structure, and a kind of fingerprint was attached to the tube surface in order to amplify the slip vibrations. Indeed, slip was observed in terms of fast oscillations in the pressure transducer voltage output, recalling the approaches described in previous sections.

## VI. ALTERNATIVE APPROACHES

Hereto, a plurality of works about the most popular techniques for the investigation of slip phenomena in artificial hands were summarized. Although some principal approaches are prominent, e.g. those resorting to contact friction or else on vibrations typical of sliding, the problem of slip detection in artificial tactile sensing can be fit into a larger framework. The following contains an exhaustive synthesis of alternative methods retrieved from literature, covering approximately the last thirty years with considerable concentration within the last ten.

### A. DIFFERENTIATION

The differentiation of the tactile signals constitutes another option to study slip. As it does neither demand multi-axial force sensors nor it does strictly depend on the presence of vibrations, we chose to classify differentiation-based methods in a distinct Section. When investigating quickly varying waveforms yielded by sliding events, the idea to calculate derivative functions might lead to useful results. Although differentiation took root in the last decade, the first attempt to attain a derived measure from tactile force sensors was done in [131]. Authors showed that a slip vector could be derived from FSR sensors mounted on a prosthetic hand. The FSR outputs, fifteen in total, were arranged into a $4 \times 4$ matrix (the missing one was considered constantly active) and their original analog values were combined arithmetically. Subtraction operations were chosen to create the derived slip vector, so that linear and twisting motion could be recognized. Movement of grasped items on a particular direction (left-right) was distinguished with elevated accuracy (94%).

Lately, a growing trend about derivative methods for slip prevention in artificial hands can be noticed. Probably, in this sense, the most recent work exploited the differentiation of the force signal collected from a CNT-based piezoresistive tactile sensor [132]. FSR force sensors, which stand in the piezoresistive domain as well, were diffusively chosen to carry out such methods; an earlier demonstration was given in [131]. In [133], a prosthetic hand was endowed with five FSR sensors (one per finger), observing the slip of various objects through the absolute value of the derivative of the FSRs signals. The grasped objects were disturbed by attaching a weight inducing vertical displacement. A fluctuating signal, resembling the filtered (and rectified) signals, was generated during the sliding phase. This allowed applying a threshold logic to produce a binary slip signal, as illustrated in a preceding work [134]. Here, the derivative was calculated on each *k-th* sample of the force signal, according to the five-point stencil. However, in [133] the average derivative of the FSRs was computed on consecutive ensembles of five points, and was coupled with the derivative of some position sensors. These were mounted on the anterior part of thumb, index and middle fingers. Non-null derivative indicated a movement of the grasped object; this information was adopted to render the slip detection procedure more robust.

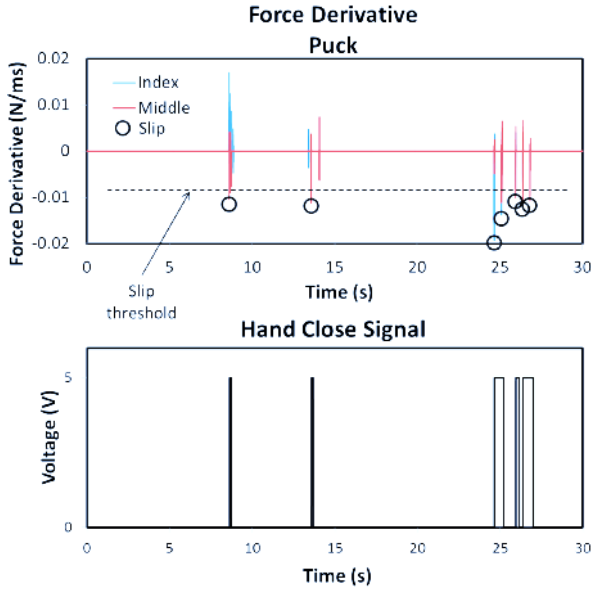


**FIGURE 10.** Grasping trial performed in [136]. Negative peaks in the derivative signal produced spikes triggering the prosthesis closure.

Moreover, combined use of more sensors was tried in [135] where a prosthetic hand (Bebionic v1) was sensorized with a strip of five barometric force sensors and one FSR force sensors. The sensors were encapsulated in a plastic cuff and fixed to the prosthesis index finger. A second-order derivative was computed on both the barometric sensors and the FSR output, i.e. normal force. Negative peaks in the derivative were observed to relate to slip of the object held by the prosthesis, while positive peaks related to mere contact. Barometric sensors showed capability to detect slip even with very small change in the force signal, having a resolution as fine as 0.001 N. Yet such sensors saturated at low pressure levels (1 N). Conversely, FSR could measure forces up to 10 N but needed greater force changes in order to recognize slip. However, the slip signals were not fed back to any controller. An almost equivalent approach was soon after presented by the same authors.([136]. It exploited only FSR sensors purposely fabricated in cuff structures and mounted on each prosthesis finger: one cuff on thumb and two on the other fingers. When a negative peak was found in the (first-order) derivative of the FSR signal, the closing action of the prosthesis (Bebionic v2) was triggered by a 100 ms wide spike. Fig. 10 plots the results of a grasping trial. In [137] the derivative of the normal force square root was computed and then evaluated through an empirical threshold. Force was measured by FSRs attached on the thumb and index of a prosthetic hand (IH2 Azzurra). Normal force was also differentiated in [88], in addition to the aforementioned filter-based technique (see above). Three-axial forces, including the normal one, were retrieved from the electrodes positioned in the biomimetic fingertip core, through a weighted sum of their outputs. As the object gripped between two biomimetic fingertips was made to slip, the derivative of the normal force component could reveal the movement of the object. Nonetheless, the differentiated normal force performed worse than the filtered pressure, though better than the IMU. This is reasonable, given that the filtered signal could rely on the microvibrations induced by the textured skin. Hence, initial slip could be detected only by the filtered pressure.

Finally, literature reports differentiation of the output of three-axial optical force sensors [138]. In this case, the derivative function was applied to the shear force. The sensor had sensing elements with conic extrusions (feelers), and was mounted on the tip of a robotic finger. Experiments were limited to the exploration of a sole parallelepiped object, and the fingertip moved along a rectangular trajectory. As the estimated shear force overcame a dual (same value with opposite sign) threshold defining a sort of band, slip was deemed to occur. Therefore, exerted force was raised up by moving the fingertip downwards.

The second derivative of the wavelength shift was studied to infer the presence of slip. Fiber Bragg Grating, included in fiber optics sensors, show a wavelength shift when a pressure is applied onto them. When the second derivative of such a shift overcame a threshold, slip was found according to the method conceived in [139].

### B. LEARNING PARADIGMS

Unlike e.g. force or position, slip has not a measurement unit as other physical quantities. The control system should decide whether to intervene in order to modify grasping parameters (e.g. fingers force or position) basing on information collected by tactile sensors. A manner to elaborate such information is to build neural networks, which are inputted with data from sensors and provide an ultimate slip signal. A neural network needs a training phase to establish the weight of its neurons; these are usually distributed in at least two layers (sometimes only one). The network is able to produce an output which is somehow linked to the input in a black box fashion. Some works employing ANN were cited earlier [63], [88], though they showed some preprocessing of the tactile signals. One of the first studies proposing to feed an ANN with unelaborated tactile data is [140], where sixteen force values were used to train a neural network whose output was defined as a *sliding coefficient* $S$. The force values were gathered from as many thin-film piezoelectric (PVDF) sensors, organized in a linear array with eight sensor couples. Each couple could measure normal stress with one sensing unit and tangential stress with the other one. The sliding coefficient approximated the ratio $T/\mu N$, with $T$, $N$ and $\mu$ denoting tangential force, normal force and friction coefficient, respectively. Hence, as the output $S$ of the ANN approached the unitary value, slip was judged to be in its incipient status. The network was trained with a back-propagation (B-P) algorithm, which is a rather common choice. For instance, B-P was used to train an ANN receiving inputs from the scattered energy emanated by slip vibrations [141]. Such an energy was estimated through a tactile stylus embedded into a robotic gripper. Additionally, the falling velocity of the grasped object acted as an input for the ANN. The optimal

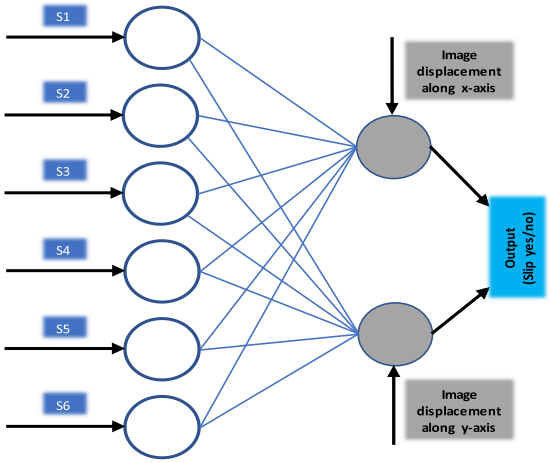


**FIGURE 11.** HN built in [144]. The S1...6 inputs from the six strain gages activated the nodes of the tactile layer. The two gray circles represent the vision nodes activated by image displacements along planar directions. The output consists in the final decision about slip occurrence.

grasping force to avoid slip, which was the output of the ANN, reached a 70% accuracy. A rather recent approach relying on B-P algorithms was presented in [142], where the ANN output again consisted in the optimal grasping force. The input for the ANN was the force ratio of (1) exerting on the distal part of the same sensorized fingertip mechanism as in [53] (see Section IIIA). A vector of force ratio values was converted into binary format, while the ANN output, with the same format, activated the actuator of the hand. The grasped objects were limited to a prism-shaped item covered with three different materials (i.e. wood, glass and spongy rubber). A neural network trained with B-P was also exploited in [143] to distinguish between sliding and slipping events in non-prehensile tasks. To this purpose, a fingertip endowed with twelve piezoresistive cells was mounted on each finger of a prosthetic hand (Shadow Hand), and their normalized output (in the range 0-1) were utilized to train the network after a preprocessing in the frequency domain. The hand was interfaced to a robotic arm, which allowed performing trials on plywood, PVC and aluminum surface. Accuracy was as high as 96.4%.

Hebbian networks (HN) found application as well in slip detection. An example is given in [144]. Here, a robotic hand was equipped with soft sensorized fingertips and a vision sensor. The former had six strain gages randomly distributed within the fingertip. The latter was a CCD camera located above the hand. The HN had two layers, i.e. one for the tactile inputs from the gages and one for the camera (Fig. 11). Initially, the HN could recognize slip as a variation occurred in the displacement between the fingertip and the contacted object. That is, slip was observable only through the camera. After a given number of learning trials, slip could be caught relying only on tactile sensors.

Learning methods go beyond ANNs. E.g., Long Short Term Memory (LSTM) networks offer a worthy solution, boasting outstanding perception of spatiotemporal correlations as proved in [145] where another camera-based sensor was experimented. The sensor was made of an elastomer, inside which some markers were located with the aim of tracking feature points. The nearest points correspondences between two consecutive frames were achieved through the K-nearest neighborhood method. Images were acquired from 3 channels, i.e. the two planar directions and magnitude, and fed to the LSTM.

Spectral analysis was combined with LSTM in [146] to process tactile data from a six-axis F/T strain-gage-based sensor, a three-axis optical force sensor, and a biomimetic fingertip hosting multiple sensors (e.g. an electrode array). Millions of sensory data were processed to effectively train slip detectors, obtaining a maximum detection time of 60 ms.

Furthermore, Gaussian Process (GP) regression was adopted to train the control of a robotic platform to avoid slip [147]. The platform had two arms, each featuring a tripod manipulator provided with a six-axis F/T sensor. The training data for the GP were the maximum linear friction force and rotational friction torque acquired by means of the F/T sensors. This approach permitted determination of torque and force limits to be exerted on a grasped object in order to prevent slip.

Recently, a multi-channel fingertip was employed to collect data used to learn some slip predictors [148]. Learning paradigms, such as support vector machines and random forest classifiers, were implemented to perform slip prediction. In [149] a Hidden Markov Model was trained to predict slip with signals acquired by means of a six-axis F/T sensor, several strain gages and PVDF sensing units.

Learning approaches guaranteed high accuracy in both grip stabilization and slip prediction, on varied objects and surfaces. Inconveniently, such approaches require huge amount of tactile data to train the learning algorithms.

## VII. DISCUSSION

The most spread methods for slip detection in artificial manipulation were presented in the sections above. Every described approach offers some advantages that led researchers to investigate the relevant potential. Nonetheless, more undeniable drawbacks prevented the adoption of a single solution and the development of a defined technology/algorithm that could impact the market. Figure 12 summarizes the strengths and weaknesses of the main methodologies employed in the effort to avoid slip.

### A. FRICTION COEFFICIENT AND MULTIAXIAL FORCES

Friction-based methods are grounded on classical physics, i.e. they are inspired by the well-known Coulomb's model of friction. Such methods were largely considered across the last twenty years of the previous century until the first years of the third millennium. A number of works studying slip as a friction-dependent problem can be found in more recent literature, though new techniques arose lastly. Friction-based algorithms, which can be implemented resorting on various

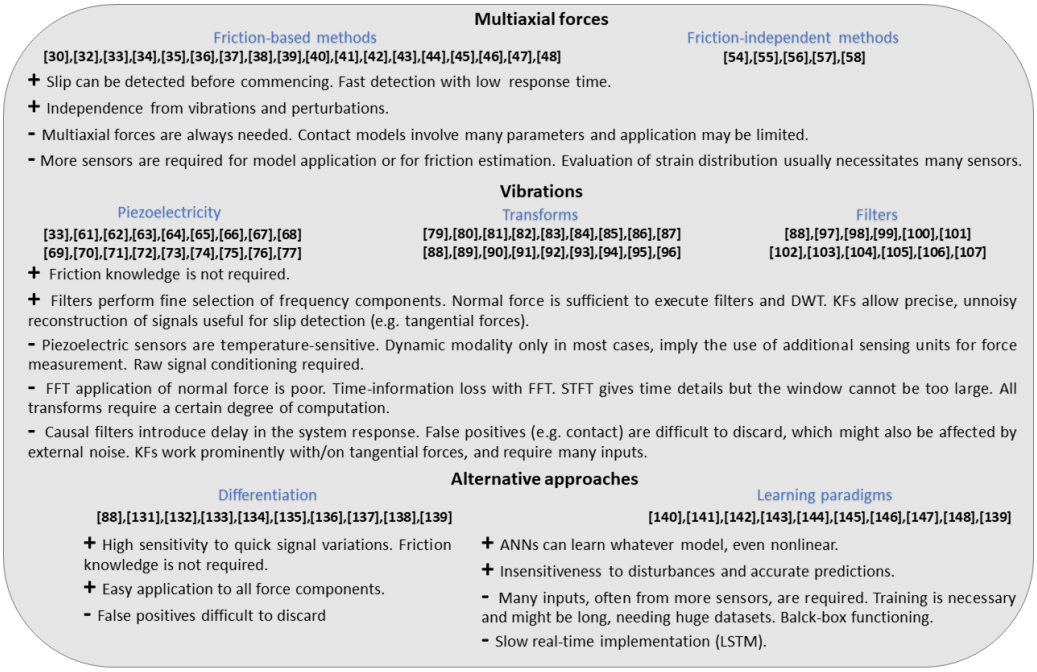


**FIGURE 12.** Summary of the main methodologies for slip detection with relevant pros and cons.

sensor technologies such as piezoresistive, capacitive, optical and QTC, allow accurate detection of slip phenomena even at the initial stage. Indeed, they provide information about the static friction coefficient of the contacted object, which directly relates to the exerted forces. By monitoring the value of the force ratio, it is possible to understand whether such a value is approaching to a limit region within which slip commences. In this situation, the tangential forces are growing, leading the grasped object to slid w.r.t. the sensor surface. Thus, opportune corrections in the grip force are to be applied, i.e. the normal force should be incremented to tighten the grip. Detecting the incipient slip allows the gripping system to correct applied force faster, as there is no need to wait for the gross phenomenon. Notwithstanding, to monitor the friction coefficient implies the use of multiaxial force sensors. At least two components of force are required in order to compute the ratio as indicated in (1). This constitutes an inconvenience also from an economic point of view, as multiaxial sensors are often more expensive than monoaxial ones. Alternatively, the friction coefficient might be estimated by means of dedicated sensors, though additional constraints can be introduced. For instance, in [51] the proposed sensor for friction coefficient estimation had to be softer than the touched object and with greater curvature, or else in [50] the friction sensor functioned along with a force sensor in order to control the pressure applied onto the grasped item. Estimation of friction coefficient may also be avoided by evaluating the strain distribution on a given surface, yet more force sensors (e.g. strain gages) are needed [55], [56].

Furthermore, the validity of Coulomb's model was brought into question since the end of the 80s [150] by the fact that its basic assumption, i.e. the proportionality between friction coefficient and normal force, is not valid for soft materials. When studying the interaction forces on a deformable surface, e.g. the compliant skin covering a robotic finger, the friction limit described in (1) should account for not only the tangential force $F_t$ but for a torsion term as well, resulting in $F_t + AM_n \leq \mu F_n$, where $M_n$ denotes an applied moment and $A$ is a constant. This formulation was demonstrated to improve robustness in predicting slip phenomena especially for what concerns soft and very soft structures [151]. Other analytical models of contact often involve supplementary parameters, besides multiaxial forces. Although the Hertzian model does not depend on friction, it necessitates other sensing units (e.g. vision sensors) to determine the radius of the contact area and the displacement of a reference point within such an area as in [44]. Mindlin's model suits better structured environments [54], as it may be applied provided that object properties (static friction coefficient above all) are known. LuGre model yields precise friction measurements despite the huge number of parameters but is mainly limited in that such measurements are satisfactory only when the object surface is quite smooth and regular [48].

### B. VIBRATIONS

Piezoelectric materials theoretically offer a high-quality solution for the development of slip sensors. This descends from their notable sensitivity to high-frequency vibrations, a property which mimics human FA II behavior. Whenever slid over a surface, the output of a piezoelectric sensor will exhibit dense fluctuations that are evident even if the sensor is slid at low velocity. This applies to all materials, regardless the

friction. Of course, the rougher is the surface, the stronger will be the piezoelectric output. On the other hand, the performance of piezoelectric sensors is affected by a certain temperature dependence; for instance, the activity of the most used piezopolymer (PVDF) in tactile systems has a variation of about 0.5%/°C [70]. Such a variability might lead to significant modification in the sensor output for abrupt temperature excursions. Despite the excellent flexibility of PVDF, this possesses low sensitivity, i.e. maximum 30 pN/C (four times less than PZT). Temperature influence on piezoelectric voltage is considered among the major shortcomings [4].

Moreover, piezoelectric signals should be properly processed before being fed back to the controller of a robotic/prosthetic hand. Given their bipolar nature, at least the signal rectification removing negative oscillations is required to prevent signal instability. This operation is usually preceded by one or more filters, which greatly help selecting a meaningful bandwidth or even to elude aliasing [64], [70]. Nonetheless, false positives associated with contact events are difficult to discard as piezoelectric sensors show sharp voltage peaks even when a contact occurs.

Due to their high frequency response, piezoelectricity-based sensors are mainly conceived to work as dynamic sensors. In fact, PVDF and PZT sensors found application in conjunction with additional sensing units devoted to force measurement [33], [61]. Piezoelectric sensors were rarely demonstrated to be able to provide both slip and force information. An example is given in [67], yet the tested force range was rather limited (1.8-7.5 N). Though piezoelectric sensors can be miniaturized and flexible, the encumbrance caused by the use of more sensors for more tactile information represents another substantial drawback.

Algorithms in the frequency domain have quite often the same objective as the ones employing piezoelectricity: to detect vibrations due to sliding movements. Analyzing the frequency of a tactile signal with transform operations such as FFT and DWT allows noticing some signal properties which are not observable if its mere time variation is studied. A considerable advantage of frequency transforms is the independence from the material friction. Indeed, as for the piezoelectric transducers, the vibrations produced by a slip event are usually at higher frequencies than static pressure signals, and this is true regardless the touched surface. However, a source of concern can be identified in the scarce applicability of FFT to normal force signals. It is well known that the most fluctuating force components during slip are the ones tangential to the surface, thus their frequency response is more powerful. This resulted e.g. in [80] where frequencies above 100 Hz could be found in tangential force, whereas in [81] a FFT peak between 1 Hz and 20 Hz was deemed as a slip. This can generate some ambiguity given that the normal force commonly shows low-frequency variation even in absence of slip. From this perspective, the DWT may be preferable over FFT as it offers superior performance on normal force as well thanks to its decomposition of the signal into approximations (low frequencies) and details (high frequencies). E.g., [91] illustrates the application of the DWT on both normal and tangential forces with comparable results, whereas examples of successful functioning on monoaxial output were provided in [94] (normal force) and [90] (monoaxial voltage). Moreover, Wavelet transform allows overcoming another widely known disadvantage implied by FFT, i.e. the loss of time information. FFT decomposes a signal into a sum of sinusoidal waves; even though this has valuable outcome in the frequency domain, it possesses no correlation between the individuated frequency components and the time domain. Diversely, DWT decomposes the signal by passing it through a series of filters which span the whole signal band, resorting on dilatations and translations of both wavelet and scaling functions. The resulting wavelet coefficients, which carry the various frequency components of the original signal, can thus be plotted on a time-scale. This is possible only in part with the STFT, which employs a fixed temporal window to create a spectrogram of the signal. Even if time information is somehow preserved in this manner, a fixed window cannot be able to detect all spectral elements of the signal. Besides, attention must be paid to the size of the window in order to keep computational times quite low. The transform-based techniques performance depends on the size of the chosen window. To perform real-time algorithms, the window should be as short as possible. For instance, in [83] such a window is 17 ms long, or else in [96] it is 21 ms long.

Computational burden must be taken into account as well, especially when a number of frequential and/or temporal features are used. As in [85], only the most significant features should be processed in order to avoid excessive slowdown in computation, which would compromise real-time operation.

The slip vibrations might also be isolated with the help of filters. They constitute an alternative to FFT and DWT as they allow obtaining a slip signal from tactile sensors output. Filters proved to perform optimally in a wide range of applications, including normal force component [101], tangential force component [98] and hydroacoustic pressured [88]. Given that slip frequencies are normally concentrated towards high values, ideal configurations are HP filters or else BP filters. An indisputable advantage of detecting slip by means of filtering functions is the unnecessity to know surface properties such as friction or roughness. Although this is shared with other techniques relying on transform operations or piezoelectric sensors, filters allow higher precision in extracting the relevant portion of the tactile signal spectrum. Indeed, such a portion can be very subtle, and is identifiable e.g. through FFT prior to the filter design [97], [98]. By combining more filters together into a network, very accurate slip signals may be achieved and used to control prosthetic hands [98] or even to generate a unique, binary slip indicator from a big number of tactile channels [100]. However, filtered signals require a certain degree of post processing, being bipolar and unstably fluctuating in their original form. Further, the implementation of filters implies the property of *causality*, which is fundamental to guarantee real-time functioning. Causal IIR filters, which depend only on past and present values of the input

signal, introduce an unavertable delay in their output. This is due to their nonlinear phase, which yields a variable distortion at different frequencies. FIR (finite impulse response) filters get around such an inconvenience as they have linear phase, though the delay in the output cannot be avoided in any case. Moreover, FIR filters need higher order to satisfy tight constraints, such as fast roll-off at the transition between pass-band and stopband. For this reason, FIR filters are not the best choice when fine bandwidth has to be privileged and fast transition band is demanded, as in the case of slip detection. In all cases, the main drawback of causal filters resides in the delay that the filtered signal will show in the time domain, which might influence negatively the performance of a filter-based method. [100], the average delay between the onset of slip and its detection was found to be lower than 50 ms. This is acceptable from a physiological point of view, yet a similar kind of analysis was rarely carried out. Consider e.g. [88]: the developed algorithms were demonstrated to identify slip faster than an IMU mounted on the grasped object, but it was not stated how fast the IMU itself could recognize slip.

Few attempts to prevent slip events by means of a particular type of filter, i.e. KF, were reported as well. KFs do provide accurate statistical measures and fit well dynamic systems, though they usually require complicated analytical procedures, and need to be fed with multiple inputs. Also, KF applications on slip detection often regarded the estimation/elaboration of tangential forces [104], [105], thus presuming the availability of multiaxial force information or even their presence in the algorithms.

### C. ALTERNATIVE APPROACHES

Differentiation was employed in the effort to figure out new slip detection methods working without knowledge of surface properties. The derivative of a force signal is computationally simple, even for a higher order than first, and permits a certain ease in the study of the variation in the tactile sensors output. At the slip moment, significant changes occur in the tactile signal; when the derivative of a force signal overcomes a given empirical threshold, slip might be identified. Successful application was shown on normal force component [134], [137], [135],.([136], on tangential force component [138] and on hydroacoustic pressure [88]. Notwithstanding, unneglectable variations happen also when the tactile sensor touches an object, i.e. when said sensor becomes active as force jumps from zero to another value. Derivative functions will exhibit correspondent peaks, which may be hard to discard without the help of other sensors. For example, [134] does not discuss the algorithm performance during contact and release phase of the prosthetic hand endowed with FSR sensors. Although the sole normal force component could be enough as an input for the derivative method, the force derivative was integrated with the derivative of position in a subsequent work [133].

Note that, in general, thresholding is widely adopted not only for differentiated signals but for e.g. transformed and filtered ones as well. It constitutes an immediate technique for the generation of binary slip signals, though thresholds are commonly determined through empiric procedures. Plus, this technique is sensitive to false positives, and authors rarely describe how to discard them.

**TABLE 2. Sensor technologies with Pros and Cons.**

| Technology | Advantages | Drawbacks |
|---|---|---|
| Optical [108],[109],[110], [111],[112],[113], [114],[115],[116], [117] | Immunity to electromagnetic disturbance<br>Independence from surface roughness<br>Very high Sensitivity | Bulky<br>Complex data elaboration<br>Typically require more than one sensing unit |
| Velocity – Acceleration [32],[71],[95], [118],[119],[120], [121],[122] | Broad frequency response<br>High sensitivity | Sensitive to external disturbances/vibrations<br>Unsuitable for static load |
| Thermal [123],[124] | Immunity to external vibrations<br>Independence from surface roughness | Unsuitable for static load<br>Long response time |
| Magnetic [125],[126],[127], [128] | Immunity to external vibrations<br>Able to sense both static and dynamic loads | Bulky<br>Performance depends on fabrication materials |

Another option for predicting slip is to adopt learning paradigms. ANNs do yield elegant implementation of slip detection strategies enabling the control system to elude ambiguities. These can derive e.g. from contact events, which might be misunderstood as slip events, or from generic noise sources (such as vibrations produced by actuators). Data with significant variability can be correctly interpreted by an ANN, that is able to learn and approximate complex, nonlinear models. Although the implementation of ANNs is theoretically simple, they usually resort on a plurality of sensory data [140], [143], often of different types [144]. From this, it derives a drawback relating to complexity. Neural networks can require huge sets of data for the training phase, which might necessitate long times. Also, more layers are commonly needed to elaborate all the available information and, as a result, the overall functioning of a neural network is viewed as a black box. That is, one knows what the network can do in terms of output but has no insights about how it actually works, in terms of information processed and exchanged by its neurons. Generally, learning paradigms still have a number of drawbacks. These range from the long training phase, slow real-time execution [148] to the large quantity of data collected from many sensing units, which are necessary for the training. However, such approaches commonly offer high-accuracy performance.

Finally, Table 2 summarizes the main advantages and disadvantages of slip detection executed with tactile sensors based on the physical quantities presented in Section IVC.

## VIII. CONCLUSION

This article surveyed the state of the art regarding slip detection with artificial tactile sensors. First, the sense of slip was described from a physiological point of view, referring to human tactile system. Next, the literature was deeply explored and a number of works were reported according to the methodology employed for the slip identification. These involved: 1) the use of multiaxial force components to study e.g. the static friction coefficient, or else of more force sensors to ensure grasp stability; 2) the piezoelectric phenomenon (exploited since the oldest attempts to provide artificial hands with slip sensors), as well as transform techniques and filters, to investigate the presence of vibrations in tactile signals; 3) the differentiation of force signals containing information associated with rapid changes occurring at the slip moment. Finally, other rather late methods, regarded with growing attention during the last decade, were presented to complete the summary of the literature. Such methods resorted on: 1) neural networks, which can predict slip if opportunely trained with tactile data; 2) physical quantities such as temperature, electromagnetic induction, light intensity and acceleration.

From a general overview, it can be stated that the methods and approaches employed to detect slip with tactile sensors cover a wide range of physical principia and technologies. Notwithstanding the number of publications in this research field exhibits a constant growth, the feeling is that a unique, generally accepted methodology has yet to be defined. For example, one may think to the first slip sensors mounted on artificial hands, which date back to half a century ago [14] and was of piezoelectric type. Though many successive attempts were done with disparate sensors and methods, piezoelectric sensors did not cease being regarded as an actual possibility, even if the number of relevant works decreased. The same applies to friction-based techniques; despite the concept of friction cone was already utilized at the end of the 80s, there are still some researchers proposing algorithms which are centered around such a concept. In other words, latest techniques were not yet able to completely convince the scientific community so far. Hence, experimental comparison among performance of classical and newer techniques is still ongoing to find out whether a real advancement subsists [116], [152]. As a matter of fact, much research is being carried out on new slip detection approaches featuring e.g. filters and DWT application. Similar approaches allow using monoaxial, low-cost sensors to perform both force and slip measurement, thus simplifying the entire process. Moreover, force calibration is not mandatory (e.g., the raw voltage can be processed). In this scenario, differentiation is also suitable but the discard of false positives must be better addressed.

According to our opinion, simplicity is a highly desirable property when attempting to endow robotic hands with tactile sensors. These should act as force sensors and slip sensors as well, in order to achieve minimal complexity and encumbrance. The impressive sensitivity and richness of information of human tactile sensors would suggest the creation of complicated sensory systems; not rarely, researchers tried to build sophisticated solutions involving more sensors and onerous computation. This might lead to greater performance but reduces the ease of applicability. The more complex is the methodology, along with the hardware required to implement it, the more difficult is expected to be the portability of said methodology and hardware. Moreover, human mechanoreceptors remain frustratingly hard to be reproduced artificially. They are of different types, specialized for diverse tasks; however, to achieve all their characteristics is not mandatory for artificial tactile sensing. Albeit physiology is for sure a great inspiration for artificial systems design, exquisite biomimicry is not crucial [16]. A complete, bio-inspired tactile system would be expected to boast a certain degree of multimodality, i.e. to provide information about temperature and humidity, besides pressure and slip. Therefore, obtaining e.g. the last two information from a unique sensing unit would be of great help, given that temperature requires an additional unit. Nonetheless, a given subset of properties may be selected depending on the application. For instance, if only the estimation of the contact force and the detection of slip are required, two different sensors can be dedicated to each of the two quantities. However, a similar procedure will always challenge designers in terms of e.g. bulkiness and power consumption. Oppositely, a single sensing unit providing at least one force component can be elaborated in such a way to infer the presence of slip, as it can be evinced from a number of works in the above Sections.

In conclusion, it can be stated that, in spite of the increasing effort produced by researchers, a gold standard solution has not been identified yet. Many approaches are still being investigated; we conjecture that a definitive convergence is quite far, as the number of relevant publications grows and possible directions appear multiple. By means of this survey, we give an overview of the heterogeneous state of the art, auspicating that it will serve as a meaningful guide for scientists and technicians involved.

## REFERENCES

[1] I. M. Bullock and A. M. Dollar, "Classifying human manipulation behavior," in *Proc. IEEE Int. Conf. Rehabil. Robot.*, Jun. 2011, pp. 1–6.
[2] R. S. Johansson and G. Westling, "Roles of glabrous skin receptors and sensorimotor memory in automatic control of precision grip when lifting rougher or more slippery objects," *Exp. Brain Res.*, vol. 56, no. 3, pp. 550–564, Oct. 1984.
[3] L. Zou, C. Ge, Z. Wang, E. Cretu, and X. Li, "Novel tactile sensor technology and smart tactile sensing systems: A review," *Sensors*, vol. 17, no. 11, p. 2653, 2017.
[4] R. S. Dahiya, G. Metta, M. Valle, and G. Sandini, "Tactile Sensing—From humans to humanoids," *IEEE Trans. Robot.*, vol. 26, no. 1, pp. 1–20, Feb. 2010.
[5] P. Dario, "Tactile sensing: Technology and applications," *Sens. Actuators A, Phys.*, vol. 26, nos. 1–3, pp. 251–256, Mar. 1991.
[6] M. H. Lee, "Tactile sensing: New directions, new challenges," *Int. J. Robot. Res.*, vol. 19, no. 7, pp. 636–643, Jul. 2000.
[7] Z. Kappassov, J.-A. Corrales, and V. Perdereau, "Tactile sensing in dexterous robot hands—Review," *Robot. Auto. Syst.*, vol. 74, pp. 195–220, Dec. 2015.

[8] H. Yousef, M. Boukallel, and K. Althoefer, "Tactile sensing for dexterous in-hand manipulation in robotics—A review," *Sens. Actuators A, Phys.*, vol. 167, no. 2, pp. 171–187, Jun. 2011.

[9] P. S. Girão, P. M. P. Ramos, O. Postolache, and J. Miguel Dias Pereira, "Tactile sensors for robotic applications," *Measurement*, vol. 46, no. 3, pp. 1257–1271, Apr. 2013.

[10] C. Chi, X. Sun, N. Xue, T. Li, and C. Liu, "Recent progress in technologies for tactile sensors," *Sensors*, vol. 18, no. 4, p. 948, 2018.

[11] A. Yamaguchi and C. G. Atkeson, "Recent progress in tactile sensing and sensors for robotic manipulation: Can we turn tactile sensing into vision?" *Adv. Robot.*, vol. 33, no. 14, pp. 661–673, Jul. 2019.

[12] A. L. Ciancio, F. Cordella, R. Barone, R. A. Romeo, A. D. Bellingegni, R. Sacchetti, A. Davalli, G. Di Pino, F. Ranieri, V. Di Lazzaro, E. Guglielmelli, and L. Zollo, "Control of prosthetic hands via the peripheral nervous system," *Frontiers Neurosci.*, vol. 10, p. 116, Apr. 2016.

[13] M. T. Francomano, D. Accoto, and E. Guglielmelli, "Artificial sense of Slip—A review," *IEEE Sensors J.*, vol. 13, no. 7, pp. 2489–2498, Jul. 2013.

[14] L. L. Salisbury and A. B. Colman, "A mechanical hand with automatic proportional control of prehension," *Med. Biol. Eng.*, vol. 5, no. 5, pp. 505–511, Sep. 1967.

[15] W. Chen, H. Khamis, I. Birznieks, N. F. Lepora, and S. J. Redmond, "Tactile sensors for friction estimation and incipient slip Detection—Toward dexterous robotic manipulation: A review," *IEEE Sensors J.*, vol. 18, no. 22, pp. 9049–9064, Nov. 2018.

[16] R. Balasubramanian and V. J. Santos, *The Human Hand as an Inspiration for Robot Hand Development*. Cham, Switzerland: Springer, 2014.

[17] A. Purves, H. Fitzpatrick, and M. LaMantia, "Williams," in *Neuroscience*, 3rd ed. Sunderland, MA, USA: Sinauer Associates, 2004.

[18] A. B. Vallbo and R. S. Johansson, "Properties of cutaneous mechanoreceptors in the human hand related to touch sensation," *Human Neurobiol.*, vol. 3, no. 1, pp. 3–14, 1984.

[19] G. Westling and R. S. Johansson, "Responses in glabrous skin mechanoreceptors during precision grip in humans," *Exp. Brain Res.*, vol. 66, no. 1, pp. 128–140, Mar. 1987.

[20] R. S. Johansson and A. B. Vallbo, "Tactile sensory coding in the glabrous skin of the human hand," *Trends Neurosciences*, vol. 6, pp. 27–32, Jan. 1983.

[21] A. Zimmerman, L. Bai, and D. D. Ginty, "The gentle touch receptors of mammalian skin," *Science*, vol. 346, no. 6212, pp. 950–954, Nov. 2014.

[22] V. Macefield and R. Johansson, "Control of grip force during restraint of an object held between finger and thumb: Responses of muscle and joint afferents from the digits," *Exp. Brain Res.*, vol. 108, no. 1, pp. 172–184, Feb. 1996.

[23] M. Knibestöl, "Stimulus-response functions of slowly adapting mechanoreceptors in the human glabrous skin area.," *J. Physiol.*, vol. 245, no. 1, pp. 63–80, 1975.

[24] M. R. Chambers, K. H. Andres, M. V. Duering, and A. Iggo, "The structure and function of the slowly adapting type II mechanoreceptor in hairy skin," *Quart. J. Experim. Physiol. Cognate Med. Sci.*, vol. 57, no. 4, pp. 417–445, Oct. 1972.

[25] R. S. Johansson and G. Westling, "Signals in tactile afferents from the fingers eliciting adaptive motor responses during precision grip," *Exp. Brain Res.*, vol. 66, no. 1, pp. 141–154, Mar. 1987.

[26] J. R. Flanagan and A. Wing, "Modulation of grip force with load force during point-to-point arm movements," *Exp. Brain Res.*, vol. 95, no. 1, pp. 131–143, Jul. 1993.

[27] J. R. Flanagan, M. C. Bowman, and R. S. Johansson, "Control strategies in object manipulation tasks," *Current Opinion Neurobiol.*, vol. 16, no. 6, pp. 650–659, Dec. 2006.

[28] G. Westling and R. S. Johansson, "Factors influencing the force control during precision grip," *Exp. Brain Res.*, vol. 53, no. 2, pp. 277–284, Jan. 1984.

[29] H. Kinoshita, L. Bäckström, J. R. Flanagan, and R. S. Johansson, "Tangential torque effects on the control of grip forces when holding objects with a precision grip," *J. Neurophysiol.*, vol. 78, no. 3, pp. 1619–1630, Sep. 1997.

[30] C. Melchiorri, "Slip detection and control using tactile and force sensors," *IEEE/ASME Trans. Mechatronics*, vol. 5, no. 3, pp. 235–243, Sep. 2000.

[31] R. Fearing, "Simplified grasping and manipulation with dextrous robot hands," *IEEE J. Robot. Autom.*, vol. 2, no. 4, pp. 188–195, Dec. 1986.

[32] M. R. Tremblay and M. R. Cutkosky, "Estimating friction using incipient slip sensing during a manipulation task," in *Proc. IEEE Int. Conf. Robot. Autom.*, May 1993, pp. 429–434.

[33] A. Mingrino, A. Bucci, R. Magni, and P. Dario, "Slippage control in hand prostheses by sensing grasping forces and sliding motion," in *Proc. IEEE/RSJ Int. Conf. Intell. Robots Syst. (IROS)*, vol. 3, Sep. 1994, pp. 1803–1809.

[34] J. L. Novak, "Initial design and analysis of a capacitive sensor for shear and normal force measurement," in *Proc. Int. Conf. Robot. Autom.*, May 1989, pp. 137–144.

[35] S. Harada, K. Kanao, Y. Yamamoto, T. Arie, S. Akita, and K. Takei, "Fully printed flexible fingerprint-like three-axis tactile and slip force and temperature sensors for artificial skin," *ACS Nano*, vol. 8, no. 12, pp. 12851–12857, Dec. 2014.

[36] T. Okatani, A. Nakai, T. Takahata, and I. Shimoyama, "A MEMS slip sensor: Estimations of triaxial force and coefficient of static friction for prediction of a slip," in *Proc. 19th Int. Conf. Solid-State Sensors, Actuat. Microsystems (TRANSDUCERS)*, Jun. 2017, pp. 75–77.

[37] L. Beccai, S. Roccella, L. Ascari, P. Valdastri, A. Sieber, M. C. Carrozza, and P. Dario, "Development and experimental analysis of a soft compliant tactile microsensor for anthropomorphic artificial hand," *IEEE/ASME Trans. Mechatronics*, vol. 13, no. 2, pp. 158–168, Apr. 2008.

[38] M. I. Tiwana, A. Shashank, S. J. Redmond, and N. H. Lovell, "Characterization of a capacitive tactile shear sensor for application in robotic and upper limb prostheses," *Sens. Actuators A, Phys.*, vol. 165, no. 2, pp. 164–172, Feb. 2011.

[39] T. Zhang, S. Fan, L. Jiang, and H. Liu, "Development and experiment analysis of anthropomorphic prosthetic hand with flexible three-axis tactile sensor," *Int. J. Hum. Robot.*, vol. 10, no. 03, Sep. 2013, Art. no. 1350028.

[40] T. Zhang, S. Fan, J. Zhao, L. Jiang, and H. Liu, "Multifingered robot hand dynamic grasping control based on fingertip three-axis tactile sensor feedback," in *Proc. 11th World Congr. Intell. Control Autom.*, Jun. 2014, pp. 3321–3326.

[41] M. Kaboli, K. Yao, and G. Cheng, "Tactile-based manipulation of deformable objects with dynamic center of mass," in *Proc. IEEE-RAS 16th Int. Conf. Hum. Robots (Humanoids)*, Nov. 2016, pp. 752–757.

[42] A. Bicchi, J. K. Salisbury, and P. Dario, "Augmentation of grasp robustness using intrinsic tactile sensing," in *Proc. Int. Conf. Robot. Autom.*, Jan. 1989, pp. 302–307.

[43] R. Bayrleithner and K. Komoriya, "Static friction coefficient determination by force sensing and its application," in *Proc. IEEE/RSJ Int. Conf. Intell. Robots Syst. (IROS)*, vol. 3, Sep. 1994, pp. 1639–1646.

[44] A. Ikeda, Y. Kurita, J. Ueda, Y. Matsumoto, and T. Ogasawara, "Grip force control for an elastic finger using vision-based incipient slip feedback," in *Proc. IEEE/RSJ Int. Conf. Intell. Robots Syst. (IROS)*, vol. 1, vol. 2004, pp. 810–815.

[45] H. Maekawa, K. Tanie, and K. Komoriya, "Tactile feedback for multifingered dynamic grasping," *IEEE Control Syst. Mag.*, vol. 17, no. 1, pp. 63–71, Feb. 1997.

[46] H. Kanno, H. Nakamoto, F. Kobayashi, F. Kojima, and W. Fukui, "Slip detection using robot fingertip with 6-axis force/torque sensor," in *Proc. IEEE Workshop Robotic Intell. Informationally Structured Space (RiiSS)*, Apr. 2013, pp. 1–6.

[47] X. Song, H. Liu, J. Bimbo, K. Althoefer, and L. D. Seneviratne, "A novel dynamic slip prediction and compensation approach based on haptic surface exploration," in *Proc. IEEE/RSJ Int. Conf. Intell. Robots Syst.*, Oct. 2012, pp. 4511–4516.

[48] X. Song, H. Liu, K. Althoefer, T. Nanayakkara, and L. D. Seneviratne, "Efficient break-away friction ratio and slip prediction based on haptic surface exploration," *IEEE Trans. Robot.*, vol. 30, no. 1, pp. 203–219, Feb. 2014.

[49] G. De Maria, C. Natale, and S. Pirozzi, "Tactile sensor for human-like manipulation," in *Proc. 4th IEEE RAS EMBS Int. Conf. Biomed. Robot. Biomechatronics (BioRob)*, Jun. 2012, pp. 1686–1691.

[50] Y. Yamada, H. Kozai, N. Tsuchida, and K. Imai, "A parallel-fingered hand system with multiple sensing functions for grasping various objects," *Adv. Robot.*, vol. 8, no. 3, pp. 321–336, Jan. 1993.

[51] H. Shinoda, S. Sasaki, and K. Nakamura, "Instantaneous evaluation of friction based on ARTC tactile sensor," in *Proc. Millennium Conf. IEEE Int. Conf. Robot. Automat. Symp. (ICRA)*, vol. 3, Apr. 2000, pp. 2173–2178.

[52] T. Okatani, H. Takahashi, K. Noda, T. Takahata, K. Matsumoto, and I. Shimoyama, "A tactile sensor using piezoresistive beams for detection of the coefficient of static friction," *Sensors*, vol. 16, no. 5, p. 718, 2016.

[53] S. M. Nacy, M. A. Tawfik, and I. A. Baqer, "A novel fingertip design for slip detection under dynamic load conditions," *J. Mech. Robot.*, vol. 6, no. 3, Aug. 2014, Art. no. 031009.

[54] Y. Ma, Y. Huang, L. Mao, P. Liu, C. Liu, and Y. Ge, "Pre-sliding detection in robot hand grasping based on slip-tactile sensor," in *Proc. IEEE Int. Conf. Robot. Biomimetics (ROBIO)*, Dec. 2015, pp. 2603–2608.

[55] Y. Koda and T. Maeno, "Grasping force control in master-slave system with partial slip sensor," in *Proc. IEEE/RSJ Int. Conf. Intell. Robots Syst.*, Oct. 2006, pp. 4641–4646.

[56] T. Maeno, T. Kawai, and K. Kobayashi, "Analysis and design of a tactile sensor detecting strain distribution inside an elastic finger," in *Proc. IEEE/RSJ Int. Conf. Intell. Robots Systems. Innov. Theory, Pract. Appl.*, Oct. 1998, pp. 1658–1663.

[57] J. A. Alcazar and L. G. Barajas, "Estimating object grasp sliding via pressure array sensing," in *Proc. IEEE Int. Conf. Robot. Autom.*, May 2012, pp. 1740–1746.

[58] M. Stachowsky, T. Hummel, M. Moussa, and H. A. Abdullah, "A slip detection and correction strategy for precision robot grasping," *IEEE/ASME Trans. Mechatronics*, vol. 21, no. 5, pp. 2214–2226, Oct. 2016.

[59] J. Baits, R. Todd, and J. Nightingale, "Paper 10: The Feasibility of an Adaptive Control Scheme for Artificial Prehension," in *Proc. Inst. Mech. Eng., Conf.*, vol. 183, no. 10. London, U.K.: SAGE, 1968, pp. 54–59.

[60] P. Dario and D. De Rossi, "Tactile sensors and the gripping challenge: Increasing the performance of sensors over a wide range of force is a first step toward robotry that can hold and manipulate objects as humans do," *IEEE Spectr.*, vol. 22, no. 8, pp. 46–53, Aug. 1985.

[61] Y. Yamada and M. R. Cutkoskv, "Tactile sensor with 3-axis force and vibration sensing functions and its application to detect rotational slip," in *Proc. IEEE Int. Conf. Robot. Autom.*, May 1994, pp. 3550–3557.

[62] Y. Xin, H. Tian, C. Guo, X. Li, H. Sun, P. Wang, J. Lin, S. Wang, and C. Wang, "PVDF tactile sensors for detecting contact force and slip: A review," *Ferroelectrics*, vol. 504, no. 1, pp. 31–45, Nov. 2016.

[63] I. Fujimoto, Y. Yamada, T. Morizono, Y. Umetani, and T. Maeno, "Development of artificial finger skin to detect incipient slip for realization of static friction sensation," in *Proc. IEEE Int. Conf. Multisensor Fusion Integr. Intell. Syst. (MFI)*, Aug. 2003, pp. 15–20.

[64] J. S. Son, E. A. Monteverde, and R. D. Howe, "A tactile sensor for localizing transient events in manipulation," in *Proc. IEEE Int. Conf. Robot. Autom.*, May 1994, pp. 471–476.

[65] J. Jockusch, J. Walter, and H. Ritter, "A tactile sensor system for a three-fingered robot manipulator," in *Proc. Int. Conf. Robot. Autom.*, vol. 4, 1997, pp. 3080–3086.

[66] B. Choi, S. Lee, H. R. Choi, and S. Kang, "Development of anthropomorphic robot hand with tactile sensor: SKKU hand II," in *Proc. IEEE/RSJ Int. Conf. Intell. Robots Syst.*, Oct. 2006, pp. 3779–3784.

[67] W. Xu, R. C. Wang, J. C. Zhang, D. W. Jin, N. Barsoum, S. Uatrongjit, and P. Vasant, "Development of a tactile and slip sensor controlled prosthetic hand system," in *Proc. AIP Conf.*, 2008, pp. 102–107.

[68] S. Shirafuji and K. Hosoda, "Detection and prevention of slip using sensors with different properties embedded in elastic artificial skin on the basis of previous experience," *Robot. Auto. Syst.*, vol. 62, no. 1, pp. 46–52, Jan. 2014.

[69] C.-H. Chuang, Y.-R. Liou, and C.-W. Chen, "Detection system of incident slippage and friction coefficient based on a flexible tactile sensor with structural electrodes," *Sens. Actuators A, Phys.*, vol. 188, pp. 48–55, Dec. 2012.

[70] D. P. J. Cotton, P. H. Chappell, A. Cranny, N. M. White, and S. P. Beeby, "A novel thick-film piezoelectric slip sensor for a prosthetic hand," *IEEE Sensors J.*, vol. 7, no. 5, pp. 752–761, May 2007.

[71] L. E. Rodriguez-Cheu and A. Casals, "Sensing and control of a prosthetic hand with myoelectric feedback," in *Proc. 1st IEEE/RAS-EMBS Int. Conf. Biomed. Robot. Biomechatronics*, Feb. 2006, pp. 607–612.

[72] L. E. Rodriguez-Cheu, D. Gonzalez, and M. Rodriguez, "Result of a perceptual feedback of the grasping forces to prosthetic hand users," in *Proc. 2nd IEEE RAS EMBS Int. Conf. Biomed. Robot. Biomechatronics*, Oct. 2008, pp. 901–906.

[73] P. Dario, R. Lazzarini, R. Magni, and S. R. Oh, "An integrated miniature fingertip sensor," in *Proc. 7th Int. Symp. Micro Mach. Hum. Sci. (MHS)*, 1996, pp. 91–97.

[74] P. H. Chappell, J. M. Nightingale, P. J. Kyberd, and M. Barkhordar, "Control of a single degree of freedom artificial hand," *J. Biomed. Eng.*, vol. 9, no. 3, pp. 273–277, Jul. 1987.

[75] P. J. Kyberd and P. H. Chappell, "Characterization of an optical and acoustic touch and slip sensor for autonomous manipulation," *Meas. Sci. Technol.*, vol. 3, no. 10, pp. 969–975, Oct. 1992.

[76] P. J. Kyberd, M. Evans, and S. te Winkel, "An intelligent anthropomorphic hand, with automatic grasp," *Robotica*, vol. 16, no. 5, pp. 531–536, Sep. 1998.

[77] D. Dornfeld and C. Handy, "Slip detection using acoustic emission signal analysis," in *Proc. IEEE Int. Conf. Robot. Autom.*, vol. 4, Mar./Apr. 1987, pp. 1868–1875.

[78] J. W. Cooley and J. W. Tukey, "An algorithm for the machine calculation of complex Fourier series," *Math. Comput.*, vol. 19, no. 90, p. 297, May 1965.

[79] E. G. M. Holweg, H. Hoeve, W. Jongkind, L. Marconi, C. Melchiorri, and C. Bonivento, "Slip detection by tactile sensors: Algorithms and experimental results," in *Proc. IEEE Int. Conf. Robot. Autom.*, vol. 4, Apr. 1996, pp. 3234–3239.

[80] R. Fernandez, I. Payo, A. Vazquez, and J. Becedas, "Micro-Vibration-Based slip detection in tactile force sensors," *Sensors*, vol. 14, no. 1, pp. 709–730, 2014.

[81] D. D. Damian, H. Martinez, K. Dermitzakis, A. Hernandez-Arieta, and R. Pfeifer, "Artificial ridged skin for slippage speed detection in prosthetic hand applications," in *Proc. IEEE/RSJ Int. Conf. Intell. Robots Syst.*, Oct. 2010, pp. 904–909.

[82] Y. Cheng, C. Su, Y. Jia, and N. Xi, "Data correlation approach for slippage detection in robotic manipulations using tactile sensor array," in *Proc. IEEE/RSJ Int. Conf. Intell. Robots Syst. (IROS)*, Sep. 2015, pp. 2717–2722.

[83] D. Goger, N. Gorges, and H. Worn, "Tactile sensing for an anthropomorphic robotic hand: Hardware and signal processing," in *Proc. IEEE Int. Conf. Robot. Autom.*, May 2009, pp. 895–901.

[84] H. Deng, G. Zhong, X. Li, and W. Nie, "Slippage and deformation preventive control of bionic prosthetic hands," *IEEE/ASME Trans. Mechatronics*, vol. 22, no. 2, pp. 888–897, Apr. 2017.

[85] I. Agriomallos, S. Doltsinis, I. Mitsioni, and Z. Doulgeri, "Slippage detection generalizing to grasping of unknown objects using machine learning with novel features," *IEEE Robot. Automat. Lett.*, vol. 3, no. 2, pp. 942–948, Apr. 2018.

[86] X. Zhang and R. Liu, "Slip detection by array-type pressure sensor for a grasp task," in *Proc. IEEE Int. Conf. Mechatronics Autom.*, Aug. 2012, pp. 2198–2202.

[87] B. Heyneman and M. R. Cutkosky, "Slip classification for dynamic tactile array sensors," *Int. J. Robot. Res.*, vol. 35, no. 4, pp. 404–421, Apr. 2016.

[88] Z. Su, K. Hausman, Y. Chebotar, A. Molchanov, G. E. Loeb, G. S. Sukhatme, and S. Schaal, "Force estimation and slip detection/classification for grip control using a biomimetic tactile sensor," in *Proc. IEEE-RAS 15th Int. Conf. Hum. Robots (Humanoids)*, Nov. 2015, pp. 297–303.

[89] K. K. Shukla and A. K. Tiwari, *Efficient Algorithms for Discrete Wavelet Transform: With Applications to Denoising and Fuzzy Inference Systems*. London, U.K.: Springer, 2013.

[90] S. Teshigawara, K. Tadakuma, A. Ming, M. Ishikawa, and M. Shimojo, "High sensitivity initial slip sensor for dexterous grasp," in *Proc. IEEE Int. Conf. Robot. Autom.*, May 2010, pp. 4867–4872.

[91] Y. Wang, K. Xi, and D. Mei, "Slip detection in prosthetic hand grasping by using the discrete wavelet transform analysis," in *Proc. IEEE Int. Conf. Adv. Intell. Mechatronics (AIM)*, Jul. 2016, pp. 1485–1490.

[92] H. Yang, X. Hu, L. Cao, and F. Sun, "A new slip-detection method based on pairwise high frequency components of capacitive sensor signals," in *Proc. 5th Int. Conf. Inf. Sci. Technol. (ICIST)*, Apr. 2015, pp. 56–61.

[93] S. Teshigawara, T. Tsutsumi, S. Shimizu, Y. Suzuki, A. Ming, M. Ishikawa, and M. Shimojo, "Highly sensitive sensor for detection of initial slip and its application in a multi-fingered robot hand," in *Proc. IEEE Int. Conf. Robot. Autom.*, May 2011, pp. 1097–1102.

[94] H. Deng, Y. Zhang, and X.-G. Duan, "Wavelet transformation-based fuzzy reflex control for prosthetic hands to prevent slip," *IEEE Trans. Ind. Electron.*, vol. 64, no. 5, pp. 3718–3726, May 2017.

[95] D. S. Chathuranga, Z. Wang, and S. Hirai, "An anthropomorphic tactile sensor system with its applications in dexterous manipulations," in *Proc. IEEE Int. Conf. Cyber Technol. Autom., Control, Intell. Syst. (CYBER)*, Jun. 2015, pp. 1085–1090.

[96] R. A. Romeo, U. B. Rongala, A. Mazzoni, D. Camboni, M. C. Carrozza, E. Guglielmelli, L. Zollo, and C. M. Oddo, "Identification of slippage on naturalistic surfaces via wavelet transform of tactile signals," *IEEE Sensors J.*, vol. 19, no. 4, pp. 1260–1268, Feb. 2019.

[97] M. Vatani, E. D. Engeberg, and J.-W. Choi, "Force and slip detection with direct-write compliant tactile sensors using multi-walled carbon nanotube/polymer composites," *Sens. Actuators A, Phys.*, vol. 195, pp. 90–97, Jun. 2013.

[98] E. D. Engeberg and S. G. Meek, "Adaptive sliding mode control for prosthetic hands to simultaneously prevent slip and minimize deformation of grasped objects," *IEEE/ASME Trans. Mechatronics*, vol. 18, no. 1, pp. 376–385, Feb. 2013.

[99] J. M. Romano, K. Hsiao, G. Niemeyer, S. Chitta, and K. J. Kuchenbecker, "Human-inspired robotic grasp control with tactile sensing," *IEEE Trans. Robot.*, vol. 27, no. 6, pp. 1067–1079, Dec. 2011.

[100] R. Romeo, C. Oddo, M. Carrozza, E. Guglielmelli, and L. Zollo, "Slippage detection with piezoresistive tactile sensors," *Sensors*, vol. 17, no. 8, p. 1844, 2017.

[101] R. Barone, A. L. Ciancio, R. A. Romeo, A. Davalli, R. Sacchetti, E. Guglielmelli, and L. Zollo, "Multilevel control of an anthropomorphic prosthetic hand for grasp and slip prevention," *Adv. Mech. Eng.*, vol. 8, no. 9, Sep. 2016, Art. no. 168781401666508.

[102] L. Zollo, G. Di Pino, A. L. Ciancio, F. Ranieri, F. Cordella, C. Gentile, and E. Noce, "Restoring tactile sensations via neural interfaces for real-time force-and-slippage closed-loop control of bionic hands," *Sci. Robot.*, vol. 4, no. 27, Feb. 2019, Art. no. eaau9924.

[103] R. Maldonado-Lopez, F. Vidal-Verdu, G. Linan, and A. Rodriguez-Vazquez, "Integrated circuitry to detect slippage inspired by human skin and artificial retinas," *IEEE Trans. Circuits Syst. I, Reg. Papers*, vol. 56, no. 8, pp. 1554–1565, Aug. 2009.

[104] N. Wettels, A. R. Parnandi, J.-H. Moon, G. E. Loeb, and G. S. Sukhatme, "Grip control using biomimetic tactile sensing systems," *IEEE/ASME Trans. Mechatronics*, vol. 14, no. 6, pp. 718–723, Dec. 2009.

[105] G. De Maria, P. Falco, C. Natale, and S. Pirozzi, "Integrated force/tactile sensing: The enabling technology for slipping detection and avoidance," in *Proc. IEEE Int. Conf. Robot. Autom. (ICRA)*, May 2015, pp. 3883–3889.

[106] A. Cavallo, G. De Maria, C. Natale, and S. Pirozzi, "Slipping detection and avoidance based on Kalman filter," *Mechatronics*, vol. 24, no. 5, pp. 489–499, Aug. 2014.

[107] S. Thrun, W. Burgard, and D. Fox, *Probabilistic Robotics*. Cambridge, MA, USA: MIT Press, 2005.

[108] S. H. Hopkins, F. Eghtedari, and D. T. Pham, "Algorithms for processing data from a photoelastic slip sensor," *Mechatronics*, vol. 2, no. 1, pp. 15–28, Feb. 1992.

[109] V. N. Dubey and R. M. Crowder, "A dynamic tactile sensor on photoelastic effect," *Sens. Actuators A, Phys.*, vol. 128, no. 2, pp. 217–224, Apr. 2006.

[110] H. William, Y. Ibrahim, and B. Richardson, "A tactile sensor for incipient slip detection," *Int. J. Optomechatronics*, vol. 1, no. 1, pp. 46–62, Mar. 2007.

[111] A. Maldonado, H. Alvarez, and M. Beetz, "Improving robot manipulation through fingertip perception," in *Proc. IEEE/RSJ Int. Conf. Intell. Robots Syst.*, Oct. 2012, pp. 2947–2954.

[112] W. Yuan, R. Li, M. A. Srinivasan, and E. H. Adelson, "Measurement of shear and slip with a GelSight tactile sensor," in *Proc. IEEE Int. Conf. Robot. Autom. (ICRA)*, May 2015, pp. 304–311.

[113] Y. Ito, Y. Kim, and G. Obinata, "Robust slippage degree estimation based on reference update of vision-based tactile sensor," *IEEE Sensors J.*, vol. 11, no. 9, pp. 2037–2047, Sep. 2011.

[114] J. W. James, N. Pestell, and N. F. Lepora, "Slip detection with a biomimetic tactile sensor," *IEEE Robot. Autom. Lett.*, vol. 3, no. 4, pp. 3340–3346, Oct. 2018.

[115] A. Gofuku, Y. Tanaka, and J. Tsubot, "Development of a flexible artificial hand system equipped with a slip sensor," *JSME Int. J. C Mech. Syst., Mach. Elements Manuf.*, vol. 43, no. 2, pp. 378–386, 2000.

[116] A. Nakagawa-Silva, N. V. Thakor, J.-J. Cabibihan, and A. B. Soares, "A bio-inspired slip detection and reflex-like suppression method for robotic manipulators," *IEEE Sensors J.*, vol. 19, no. 24, pp. 12443–12453, Dec. 2019.

[117] H. Khamis, B. Xia, and S. J. Redmond, "A novel optical 3D force and displacement sensor–Towards instrumenting the PapillArray tactile sensor," *Sens. Actuators A, Phys.*, vol. 291, pp. 174–187, Jun. 2019.

[118] N. Morita, H. Nogami, Y. Hayashida, E. Higurashi, T. Ito, and R. Sawada, "Development of a miniaturized laser Doppler velocimeter for use as a slip sensor for robot hand control," in *Proc. 28th IEEE Int. Conf. Micro Electro Mech. Syst. (MEMS)*, Jan. 2015, pp. 748–751.

[119] R. D. Howe and M. R. Cutkosky, "Sensing skin acceleration for slip and texture perception," in *Proc. Int. Conf. Robot. Autom.*, 1989, pp. 145–150.

[120] M. Tremblay, W. Packard, and M. Cutkosky, "Utilizing sensed incipient slip signals for grasp force control," Center Des. Res., Stanford Univ., Stanford, CA, USA, 1992.

[121] V. Abhinav and S. Vivekanandan, "Real-Time intelligent gripping system for dexterous manipulation of industrial Robots," in *Proc. World Congr. Eng.*, vol. 2, 2009, pp. 1–6.

[122] P. Weiner, C. Neef, Y. Shibata, Y. Nakamura, and T. Asfour, "An embedded, multi-modal sensor system for scalable robotic and prosthetic hand fingers," *Sensors*, vol. 20, no. 1, p. 101, 2020.

[123] D. Accoto, R. Sahai, F. Damiani, D. Campolo, E. Guglielmelli, and P. Dario, "A slip sensor for biorobotic applications using a hot wire anemometry approach," *Sens. Actuators A, Phys.*, vol. 187, pp. 201–208, Nov. 2012.

[124] M. T. Francomano, D. Accoto, E. Morganti, L. Lorenzelli, and E. Guglielmelli, "A microfabricated flexible slip sensor," in *Proc. 4th IEEE RAS EMBS Int. Conf. Biomed. Robot. Biomechatronics (BioRob)*, Jun. 2012, pp. 1919–1924.

[125] S. Takenawa, "A magnetic type tactile sensor using a two-dimensional array of inductors," in *Proc. IEEE Int. Conf. Robot. Autom.*, May 2009, pp. 3295–3300.

[126] M. Goka, H. Nakamoto, and S. Takenawa, "A magnetic type tactile sensor by GMR elements and inductors," in *Proc. IEEE/RSJ Int. Conf. Intell. Robots Syst.*, Oct. 2010, pp. 885–890.

[127] Y. Liu, H. Han, T. Liu, J. Yi, Q. Li, and Y. Inoue, "A novel tactile sensor with electromagnetic induction and its application on stick-slip interaction detection," *Sensors*, vol. 16, no. 4, p. 430, 2016.

[128] T. Kawamura, N. Inaguma, K. Nejigane, K. Tani, and H. Yamada, "Measurement of slip, force and deformation using hybrid tactile sensor system for robot hand gripping an object," *Int. J. Adv. Robot. Syst.*, vol. 10, no. 1, p. 83, Jan. 2013.

[129] D. Gunji, T. Araki, A. Namiki, A. Ming, and M. Shimojo, "Grasping force control of multi-fingered robot hand based on slip detection using tactile sensor," *J. Robot. Soc. Jpn.*, vol. 25, no. 6, pp. 970–978, 2007.

[130] D. Gong, R. He, J. Yu, and G. Zuo, "A pneumatic tactile sensor for co-operative robots," *Sensors*, vol. 17, no. 11, p. 2592, 2017.

[131] P. J. Kyberd and P. H. Chappell, "Object-slip detection during manipulation using a derived force vector," *Mechatronics*, vol. 2, no. 1, pp. 1–13, Feb. 1992.

[132] J.-K. Lee, H.-H. Kim, J.-W. Choi, K.-C. Lee, and S. Lee, "Development of direct-printed tactile sensors for gripper control through contact and slip detection," *Int. J. Control, Autom. Syst.*, vol. 16, no. 2, pp. 929–936, Apr. 2018.

[133] C. F. Pasluosta and A. W. L. Chiu, "Evaluation of a neural network-based control strategy for a cost-effective externally-powered prosthesis," *Assistive Technol.*, vol. 24, no. 3, pp. 196–208, Sep. 2012.

[134] C. F. Pasluosta, H. Tims, and A. W. L. Chiu, "Slippage sensory feedback and nonlinear force control system for a low-cost prosthetic hand," *Amer. J. Biomed. Sci.*, vol. 1, no. 4, pp. 295–302, Oct. 2009.

[135] L. Osborn, N. V. Thakor, and R. Kaliki, "Utilizing tactile feedback for biomimetic grasping control in upper limb prostheses," in *Proc. IEEE SENSORS*, Nov. 2013, pp. 1–4.

[136] L. Osborn, W. W. Lee, R. Kaliki, and N. Thakor, "Tactile feedback in upper limb prosthetic devices using flexible textile force sensors," in *Proc. 5th IEEE RAS/EMBS Int. Conf. Biomed. Robot. Biomechatronics*, Aug. 2014, pp. 114–119.

[137] F. Cordella, C. Gentile, L. Zollo, R. Barone, R. Sacchetti, A. Davalli, B. Siciliano, and E. Guglielmelli, "A force-and-slippage control strategy for a poliarticulated prosthetic hand," in *Proc. IEEE Int. Conf. Robot. Autom. (ICRA)*, May 2016, pp. 3524–3529.

[138] M. Ohka, J. Takata, H. Kobayashi, H. Suzuki, N. Morisawa, and H. B. Yussof, "Object exploration and manipulation using a robotic finger equipped with an optical three-axis tactile sensor," *Robotica*, vol. 27, no. 05, p. 763, Sep. 2009.

[139] J. Feng and Q. Jiang, "Slip and roughness detection of robotic fingertip based on FBG," *Sens. Actuators A, Phys.*, vol. 287, pp. 143–149, Mar. 2019.

[140] G. Canepa, R. Petrigliano, M. Campanella, and D. De Rossi, "Detection of incipient object slippage by skin-like sensing and neural network processing," *IEEE Trans. Syst., Man Cybern., B (Cybern.)*, vol. 28, no. 3, pp. 348–356, Jun. 1998.

[141] A. M. Mazid and M. F. Islam, "Grasping force estimation recognizing object slippage by tactile data using neural network," in *Proc. IEEE Conf. Robot., Autom. Mechatronics*, Sep. 2008, pp. 935–940.

[142] S. M. Nacy, M. A. Tawfik, and I. A. Baqer, "A novel approach to control the robotic hand grasping process by using an artificial neural network algorithm," *J. Intell. Syst.*, vol. 26, no. 2, pp. 215–231, Jan. 2017.

[143] M. Meier, G. Walck, R. Haschke, and H. J. Ritter, "Distinguishing sliding from slipping during object pushing," in *Proc. IEEE/RSJ Int. Conf. Intell. Robots Syst. (IROS)*, Oct. 2016, pp. 5579–5584.

[144] K. Hosoda, Y. Tada, and M. Asada, "Internal representation of slip for a soft finger with vision and tactile sensors," in *Proc. IEEE/RSJ Int. Conf. Intell. Robots Syst.*, vol. 1, Sep. 2002, pp. 111–115.

[145] Y. Zhang, Z. Kan, Y. Alexander Tse, Y. Yang, and M. Yu Wang, "FingerVision tactile sensor design and slip detection using convolutional LSTM network," 2018, *arXiv:1810.02653*. [Online]. Available: http://arxiv.org/abs/1810.02653

[146] K. Van Wyk and J. Falco, "Calibration and analysis of tactile sensors as slip detectors," in *Proc. IEEE Int. Conf. Robot. Autom. (ICRA)*, May 2018, pp. 2744–2751.

[147] F. E. Vina B, Y. Bekiroglu, C. Smith, Y. Karayiannidis, and D. Kragic, "Predicting slippage and learning manipulation affordances through Gaussian process regression," in *Proc. 13th IEEE-RAS Int. Conf. Hum. Robots (Humanoids)*, Oct. 2013, pp. 462–468.

[148] F. Veiga, J. Peters, and T. Hermans, "Grip stabilization of novel objects using slip prediction," *IEEE Trans. Haptics*, vol. 11, no. 4, pp. 531–542, Oct. 2018.

[149] N. Jamali and C. Sammut, "Slip prediction using hidden Markov models: Multidimensional sensor data to symbolic temporal pattern learning," in *Proc. IEEE Int. Conf. Robot. Autom.*, May 2012, pp. 215–222.

[150] R. D. Howe, I. Kao, and M. R. Cutkosky, "The sliding of robot fingers under combined torsion and shear loading," in *Proc. IEEE Int. Conf. Robot. Autom.*, Apr. 1988, pp. 103–105.

[151] M. R. Cutkosky and P. K. Wright, "Friction, stability and the design of robotic fingers," *Int. J. Robot. Res.*, vol. 5, no. 4, pp. 20–37, Dec. 1986.

[152] J. Reinecke, A. Dietrich, F. Schmidt, and M. Chalon, "Experimental comparison of slip detection strategies by tactile sensing with the BioTac on the DLR hand arm system," in *Proc. IEEE Int. Conf. Robot. Automat. (ICRA)*, May 2014, pp. 2742–2748.